



**Flinders**  
UNIVERSITY

Organic Diodes Towards  
Radio Frequency Identification

Ashley H. Johns BSc(Nano)Hons.

Supervisors: Prof. D.A. Lewis and Prof. J. Quinton

This thesis is submitted as a requirement pertaining to the Degree of Masters of Chemistry at the School of Chemical and Physical Sciences of Flinders University of South Australia.

Submission Date: 31/08/2015

## 2. Table of Contents

1. Title Page.....	i
2. Table of Contents.....	ii
3. Introduction .....	1
3.1. Radio Frequency Identification Systems.....	1
3.1.1. RFID Tag Structure.....	2
3.1.2. Rectification Circuits .....	3
3.2. Inorganic Electronics.....	5
3.2.1. p-n Junctions .....	5
3.2.2. Schottky Diode.....	7
3.2.3. Metal-Semiconductor Junction .....	7
3.3. Organic Electronics .....	9
3.3.1. n-type Organic Semiconductors.....	10
3.3.2. p-type Organic Semiconductors.....	11
3.3.3. Charge Transfer Complex.....	11
3.3.4. Poly(3-hexylthiophene-2,5-diyl), (P3HT) .....	12
3.4. Organic Diode Characterisation .....	15
3.4.1. Schottky Characterisation .....	15
3.5. Organic Diode Applications.....	20
3.5.1. Solution Processed Diodes.....	21
4. Experimental.....	24
4.1. Fabrication.....	24
4.1.1. Fabrication Parameters of Devices .....	24
4.1.2. Device Fabrication Recipe.....	25
4.1.3. Device Fabrication in Air.....	26
4.1.4. Device Fabrication in Inert Atmosphere.....	27

4.1.5.	Metal Electrode Evaporation .....	29
4.2.	Electrical Characterisation .....	30
5.	Results and Discussion .....	32
5.1.	Equivalent Circuit Simulation and Electrical Characterisation.....	32
5.1.1.	Equivalent Circuit Simulation.....	32
5.1.2.	Impact of Series (R1) and Shunt (R2) resistance.....	33
5.1.3.	Open Circuit Sweep Test of Kiethley 2400 .....	34
5.1.4.	Device Testing Protocol Development .....	36
5.1.5.	Photodiode Properties of P3HT Diodes .....	38
5.2.	Electrical Parameters of Diodes in Ambient, Inert and Controlled Environments ...	39
5.2.1.	Fabrication of Devices in Ambient Air.....	39
5.2.2.	Fabrication of Devices in an Inert Environment.....	50
5.2.3.	Controlled Environment Device Testing .....	56
5.3.	Device Parameters.....	62
5.3.1.	Diode Area .....	62
5.3.2.	P3HT Layer Thickness .....	65
5.4.	Rectification .....	72
5.4.1.	Half Wave Rectifier .....	73
6.	Conclusions .....	77
7.	References .....	80

## Abstract

The diode fabrication parameters were the primary focus of this project and their influence on the electrical properties of the diodes. The testing conditions and method have also been investigated because they have an impact on the electrical properties. Specific electrical properties investigated were series resistance, shunt resistance, rectification ratio and ideality.

The primary driver for this project was to overcome the affordability issues of RFID tags. RFID tags require ICs (integrated circuit) for power rectification and data processing. The ICs are the basis of RFID technology but have reached a limit of minimum cost due to the expensive manufacturing techniques. Printable OSCs (Organic Semiconductor)s are posed as an excellent alternative, in particular soluble conductive polymers lend themselves to a variety of printing techniques. Although transistors receive much of the focus of OSC research, diodes are just as important in RFID devices, particularly rectification circuits. There are many challenges to be overcome before organic electronics can be produced for the commercial market, particularly for RFID. Some challenges include, low mobility, capacitance effects at high frequencies, refinement of fabrication techniques and sheet resistance. All of these areas warrant research effort to realise OSC as diodes in RFID logic and rectification circuits.

The fabrication method of the diodes developed as the project progressed. When a reproducible method was developed, different variables were altered to investigate the effect on the electrical parameters. The parameters were then extracted from the J-V characteristic curves.

Two fabricated diodes were incorporated as the active component in half-wave rectifier circuits. The circuits successfully rectified alternating current into half-wave current. Through appropriate choice of components direct current could have been realised.

The main result was an OSC diode with a rectification of  $\sim 7.5 \times 10^5 : 1$  which is still a long way from crystalline inorganic Schottky diodes that typically have a rectification ratio in the range of 100,000,000,000:1. An exceptionally significant result was the effect of the drying time, between spin coating a sample and annealing the sample. Diodes with drying time less than 1 minute performed poorly; whereas diodes with drying time greater than 6 minutes performed exceptionally well.

## Declaration

I certify that this thesis does not incorporate without acknowledgement any material previously submitted for a degree or diploma in any university; and that to the best of my knowledge and belief it does not contain any material previously published or written by another person except where due reference is made in the text.

Signed Ashley H. Johns \_\_\_\_\_

## Acknowledgements

I would like to thank the following people:

Professor David Lewis for his seemingly infinite knowledge, guidance and challenging myself as a scientist. I feel he has significantly helped improve my skills as a professional scientist.

Professor Jamie Quinton for his encouragement, support and advice during the project, for the project and generally life related.

My wife Amanda, without her I wouldn't be the person I am today. I have never met someone so consistently determined and strong-minded despite the adversity she has faced and is a constant source of inspiration to me. She motivates me to be a better person every day.

I would especially like to thank my family for their understanding and unwavering support and encouragement; my father for being the inspiration for aspiration to achieve; my mother who has and continues to pass on worldly knowledge and encourage me to question everything and last but not least my brother who I love and trust implicitly.

The research group have been a great source of information, critique and support during my project. I have made some good friends and met some interesting people that have all enriched my life.

## Glossary of Abbreviations within the Text

Abbreviation	Definition
AC	Alternating Current
AFM	Atomic Force Microscope
DC	Direct Current
DCB	1,2 - Dichlorobenzene
EEPROM	Electrically Erasable Programmable Read - Only Memory
FET	Field Effect Transistor
FRAM	Ferroelectric Random Access Memory
IC	Integrated Circuit
I	Current
I-V	Current – Voltage
J	Current Density
J-V	Current Density - Voltage
OSC	Organic Semiconductor
PEDOT	Poly(3,4-ethylenedioxythiophene)
P3HT	Poly(3-hexylthiophene-2,5-diyl)
PSS	Polystyrenesulfonate
PVD	Physical Vapour Deposition
RAM	Random Access Memory
ROM	Read Only Memory
$R_{\text{shunt}}$	Shunt Resistance

$R_{\text{Series}}$	Series Resistance
RFID	Radio Frequency IDentification
RMS	Root Mean Square
SCE	Standard Calomel Electrode
TGA	Thermo-Gravimetric Analysis
UV-Vis	Ultra Violet – Visible

# 3. Introduction

## 3.1. *Radio Frequency Identification Systems*

The term Radio Frequency Identification or RFID describes systems that rely on electromagnetic waves from the “radio” spectrum (30 kHz to 300 GHz) as a communication medium for identification and monitoring of units within a system. RFID systems are composed of interrogators (readers) and tags (labels). An RFID reader is similar to a barcode scanner with the exception that radio-waves are used to interrogate the tag as opposed to a laser to read a barcode. The information is then either interpreted by the reader or sent directly to a main computer to be interpreted and analysed. Some readers can also program RFID tags.

A common example is EZPass, a system for paying road tolls to reduce the amount of toll booth attendees that need to work at the toll plaza, while massively increasing the flow of cars by avoid stopping and physically exchange money. The driver’s information is held on an EZPass tag that is placed on their windshield - a triggering request is made from the toll point using radio-signals to an RFID reader in the vehicle which responds with personalised encoded information identifying the RFID tag. The toll gates’ main computers then debit the account of the registered user for the amount of the toll.

RFID tags come in many shapes and sizes, the largest can weigh up to a kilogram, cost hundreds of dollars and have a detection range of many kilometres. The smallest commercial tags were mass produced (500 Million) for Gillette for 15c each[1]. If RFID is to be implemented for every item (for example in a supermarket), the price of each tag must be only a small percentage of the products price; although 15c per tag appears to be cheap however this value would preclude the use on most products in a supermarket. The most expensive part of an RFID tag is the integrated circuit (IC) or “chip”, which is based on silicon technology, and provides the greatest opportunity to reduce the price when replaced with printed organic semiconductors.

### 3.1.1. RFID Tag Structure

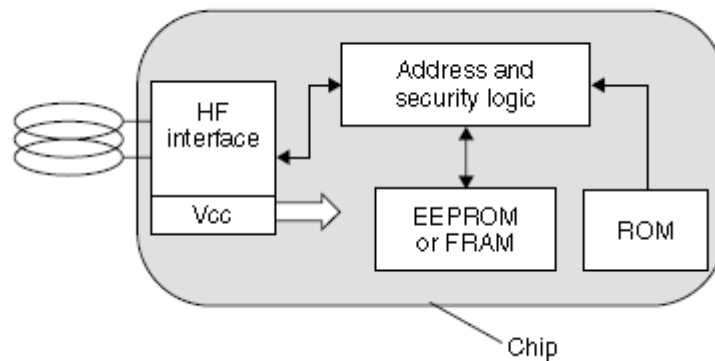


Figure 1. Block diagram of an RFID integrated circuit.

The integrated circuits or ‘chips’ are the “brains” of the RFID tag. It has a number of circuits including the HF (High Frequency) interface, memory storage, address logic and security logic. All of these circuits are made up of electrical components and shown in Figure 1.

RFID tags employ an aerial to receive and send signals to and from RFID readers. The size and shape of the tag’s aerial will depend on the application of the tag and the frequency of the radiation. The block diagram above describes the general structure of an RFID tag.

Tags with a memory function range from the simple read-only transponder to the high end transponder with cryptologic functions. Tags with a memory function contain RAM, ROM, EEPROM or FRAM. The main distinguishing characteristic of this family of tags is the use of address and security logic on the chip using a state machine.

Tags are either Active (self-powered) or Passive, where the energy is generated from the interrogating RF signal. Active tags use an inbuilt battery to supply power directly to the device. Active tags will reside in a state of low power consumption until the detection circuit activates the tag when a signal is received.

Passive tags do not have their own power supply, and are supplied with energy via the HF field of the reader. To achieve this, the HF interface draws current from the tags antenna, which is rectified and supplied to the chip as a regulated supply voltage. The HF also performs the same functions of a classical modem (modulator–demodulator) used for analogue data transmission via telephone lines, interfacing between the digital circuitry and the analogue, high frequency transmission from the reader to the tag. To perform demodulation and supply power the HF interface requires a rectification circuit.

RFID Tag ICs are composed of electrical components (wires, resistors, transistors, etc). These components are found in common ICs and are defined by their electrical properties. The two defining properties are directionality and gain. Directionality of an electrical component means whether the flow of electricity is the same in one direction as the opposite direction. A component with gain has the ability to increase the magnitude of an input signal. Gain specifically is the ratio of output/input signals magnitude.

Passive electrical components do not have directionality or gain. They include interconnects (wires), resistors, inductors and capacitors. Passive components are comparatively simple to make compared to active components.

Active electrical components have directionality and or gain properties. Included in this group are optoelectronic devices, transistors and diodes. The majority of components are based on semiconductor technology. The most essential component of the power supply on a RFID chip is the rectifier which is most commonly made from diodes.

A diode, by definition, is a two electrode device allowing current to move through it in one direction with far greater ease than the opposite direction. Diodes rely on semiconductor technology to perform their function. There are many different types of diodes but the two most common in rectifiers are the p-n junction and the Schottky diode.

### **3.1.2. Rectification Circuits**

Diodes are the primary means to rectify or convert an Alternating Current (AC) to Direct Current (DC). Half-wave rectifiers are the simplest type of rectification circuit which can be composed of a single diode - these rectifiers are named as such because they will output only the positive phase, which is half of the AC signal.

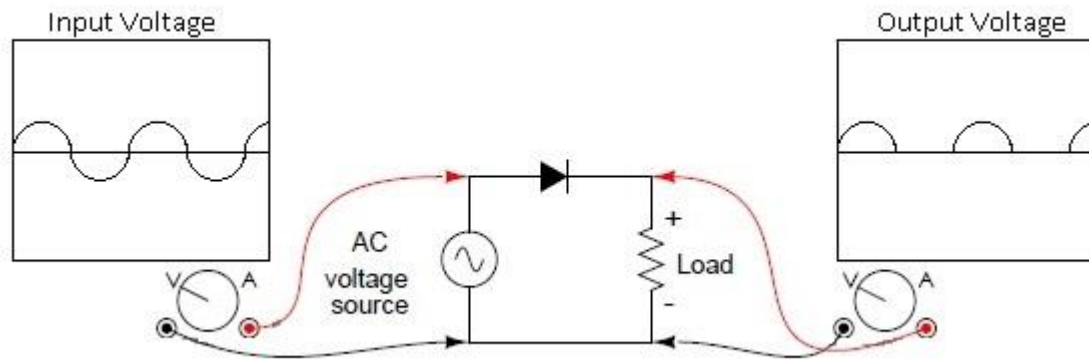


Figure 2. Half-wave rectifier with input and output voltmeters

Half-wave rectifiers are insufficient for most power supply applications, as the harmonic content of the output waveform is very difficult to filter; furthermore the half-wave rectifier transfers only half of the power from the source to the load (Figure 2). Full-wave rectifiers are more complex and require four diodes but result in both the positive and negative phase of the AC to be rectified into DC current (Figure 3).

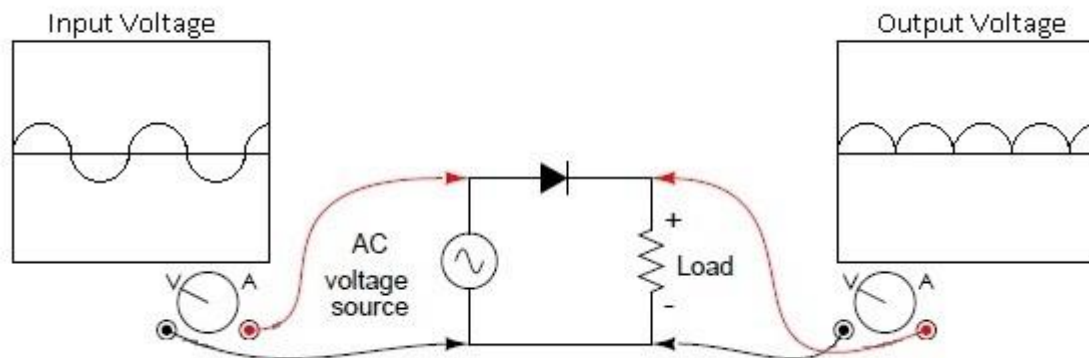


Figure 3. A Full-wave bridge rectifier with input and output voltmeters.

The output voltage of half- and full-wave can be smoothed to a constant voltage by the addition of resistors and capacitors to the circuit to form an RC filter.

## **3.2. Inorganic Electronics**

Inorganic semiconductors are made from doped crystalline Silicon or Germanium boules. Intrinsic semiconductors have a full valence band and empty conduction band which results in poor semiconducting properties. Boules are cut into wafers which are further doped with atoms that act as electron donors or acceptors to produce extrinsic semiconductors. Methods of doping include vapour-phase epitaxy, ion implantation and with low concentrations of atoms to create the semiconducting circuits. For silicon, dopants from Group V elements such as phosphorus result in extra valence electrons that are delocalised which cause the area to be electrically conductive n-type semiconductor. Dopants from Group III are missing a valence electron and act as acceptors creating a hole which can move through the lattice resulting in a p-type semiconductor. Due to the highly ordered nature of the crystalline silicon, well defined work-functions and electronic bands can be produced precisely with very fine structures.

### **3.2.1. p-n Junctions**

The foundation of semiconductor devices is based on the theory of current-voltage characteristics of p-n junctions established by Shockley[2], these junctions are of great importance in understanding other semiconductor devices and their modern applications. A p-n junction is named after the construction of the diode, the p and n refer to the two semiconductor layers, the n-type semiconductor layer the majority of charge carriers are electrons, conversely the p-type semiconductor layer's majority of charge carriers are "holes" which are the conceptual opposite of electrons. At the junction of the two semiconductor layers the electrons (in the n-type layer) and holes (in the p-type layer) will move to the opposite layer to equilibrate the charge forming an area called the depletion region, the simplest approximation of a depletion region is of an abrupt junction where the two layers have an abrupt interface.

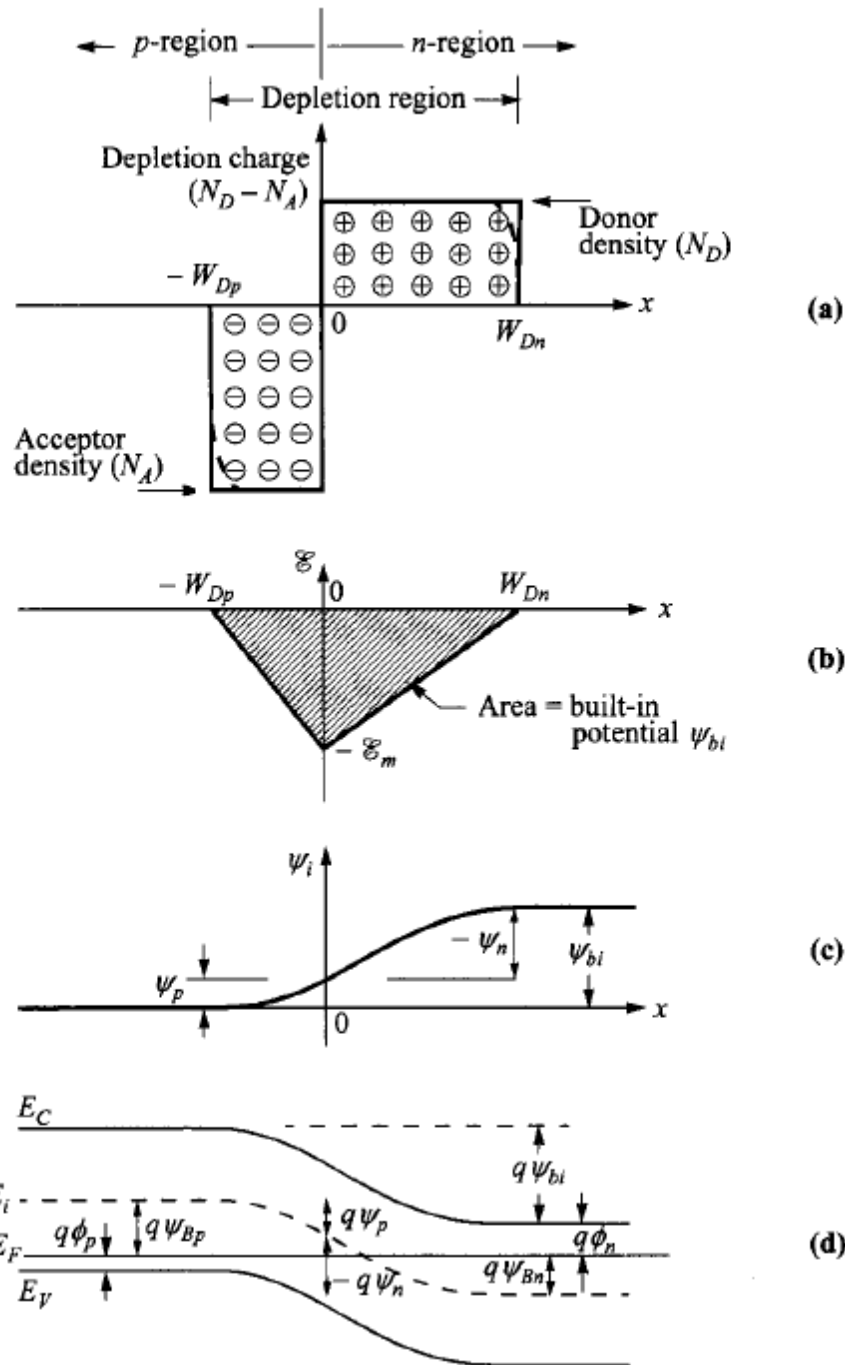


Figure 4. Abrupt p-n junction at thermal equilibrium. (a) Space-charge distribution. (b) Electric-field distribution. (c) Potential distribution (d) Energy-band diagram.[3]

The charge density of each layer will affect the width of the depletion region and the proportion of each layer in which it resides (Figure 4 (a) and (b)). The depletion region causes the built-in potential to be formed in Figure 4 (c) where an electron at position  $x$  will require the built-in potential to diffuse across the depletion region. In terms of energy levels, at thermal equilibrium the Fermi-levels of each layer become aligned and the built-in potential is the difference between the Fermi-levels Figure 4 (d). Depending on the device

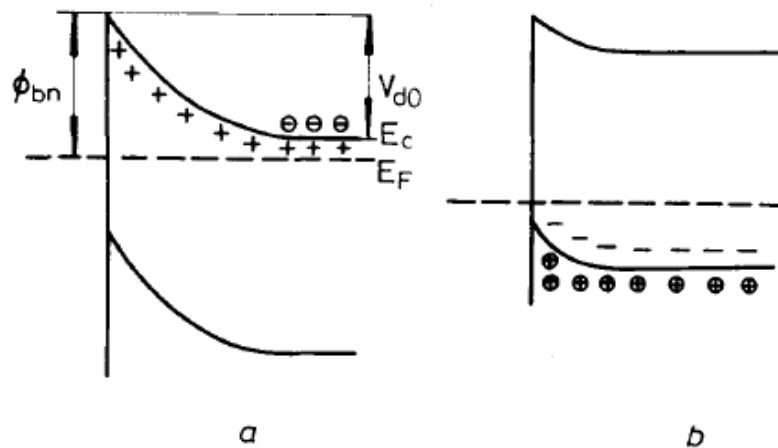
geometry, biasing condition and doping profile, a p-n junction can perform a range of functions. The theory of these junctions can be applied to many other junctions including metal-semiconductor junctions.

### 3.2.2. Schottky Diode

Schottky diodes are constructed of a metal-to-semiconductor junction rather than a p-n semiconductor junction. Also known as hot-carrier diodes, Schottky diodes have advantages over p-n junctions including: fast switching times (low reverse-recovery time), low junction capacitance, low forward voltage drop (typically 0.25 to 0.4 volts for a metal-silicon junction), and low transient reverse current during switching making them ideal for use in rectification circuits.

### 3.2.3. Metal-Semiconductor Junction

Metal-Semiconductor junctions are much simpler than p-n junctions. An electrostatic barrier is formed between the metal and semiconductor due to the difference between the work functions of the two materials. Depending on the work functions of the metal and the band-gap of the semiconductor involved a metal-semiconductor can form a Schottky diode.



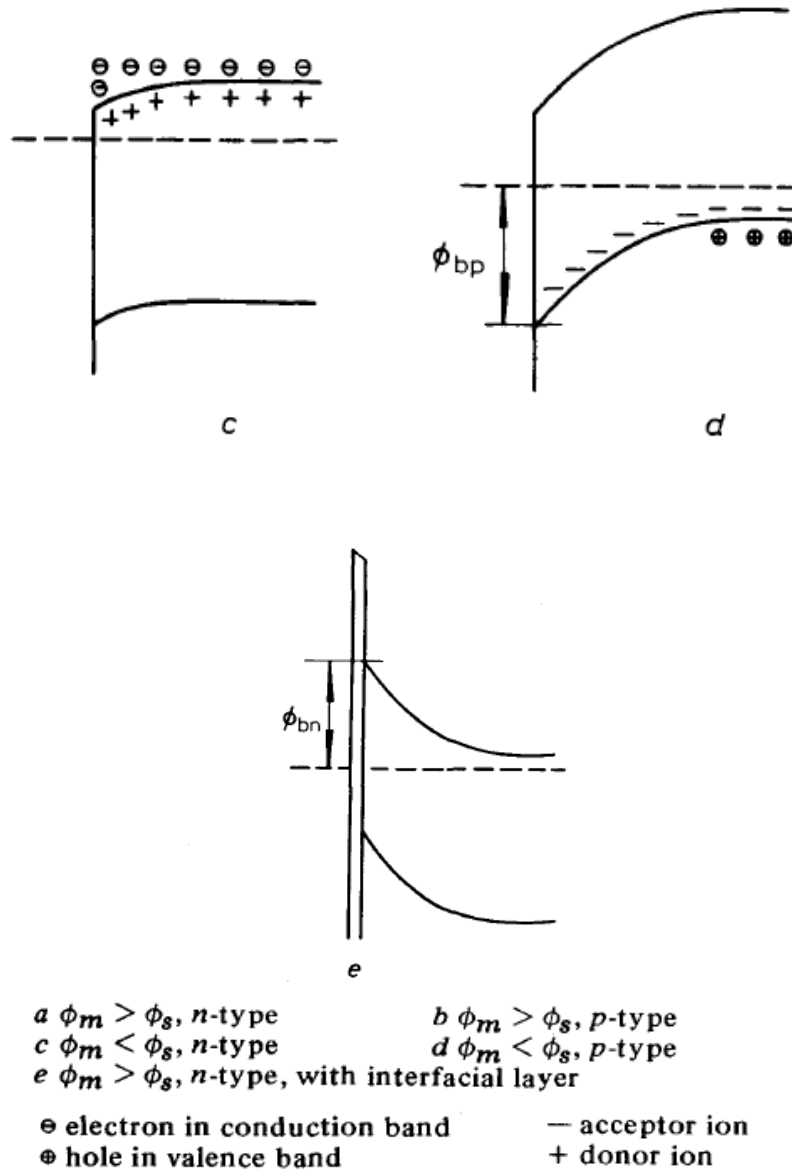


Figure 5. A Summary of metal-semiconductor interfaces at zero bias. [4]

Where  $\phi_m$  is the work-function of the metal and  $\phi_s$  is the work-function of the semiconductor. For the cases in Figure 5 b) and c), Ohmic contacts will be formed because there is no impediment to the major charge carriers, hence no rectification will occur. Cases in Figure 5 a) and d), a Schottky contact will be formed where a rectifying junction will occur.

### 3.3. Organic Electronics

The origin of organic semiconductors can be traced back to the discovery of electrical conduction in aromatic compound single crystals in the 1950's[5]. Discovery of the conductive properties of polyacetylene occurred in the early 1970s when Park Yung-woo a visiting researcher from South Korea supervised by Professor Hideki Shirakawa accidentally polymerized acetylene with 1000 times the required amount of catalyst. The resultant polyacetylene was a silver, conductive film. Shirakawa later collaborated with physicist Alan J. Heeger and chemist Alan G MacDiarmid, and discovered in 1976 that oxidation of this material with iodine results in a  $10^8$  - fold increase in conductivity[6]. The conductivity of this doped material can approach the conductivity of the best available conductor, silver. While similar highly-conductive polymers had been reported before, this was one of the first known examples of a semiconducting organic polymer. The three were awarded the Nobel Prize in Chemistry in 2000 for their discoveries[7]. Since then it has been a popular choice for diode experiments in many forms including doped, functionalised, as a composite or a doped composite.

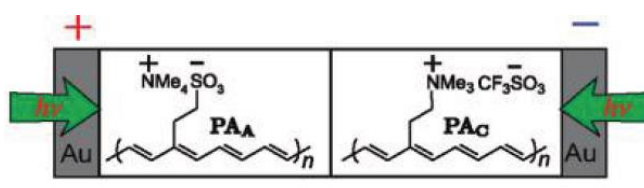


Figure 6. The sandwich structure of a polyacetylene organic semiconductor p-n junction diode.

Organic semiconductors can be small molecules, such as the aromatic compounds, or polymers. Small molecule organic semiconductors are separate conductive organic molecules which form a crystalline structure. The crystalline nature results in the formation of a valence and conduction band similar to the silicon crystal. Conjugated polymers are 'molecular' analogues of inorganic semiconductors, which commonly conduct via the delocalised electron cloud. Conjugation of a polymer is the alternation of double and single carbon-carbon bonds along the backbone of the polymer which results in overlap of the  $\pi$ -orbitals and results in the delocalisation of electrons. Organic semiconductors are intrinsic semiconductors due to the delocalised  $\pi$ -electron cloud which forms a band gap[8].

Depending on doping, the electronic levels (HOMO and LUMO) of the band gap will define what type (p or n) semiconductor will result such as the polyacetylene in Figure 6. The amorphous structure results in broadening of the energy bands[8] in Figure 7. A combination

of amorphous and crystalline structures and broadening of the energy levels cause the electrical properties to vary in polymeric semiconductors.

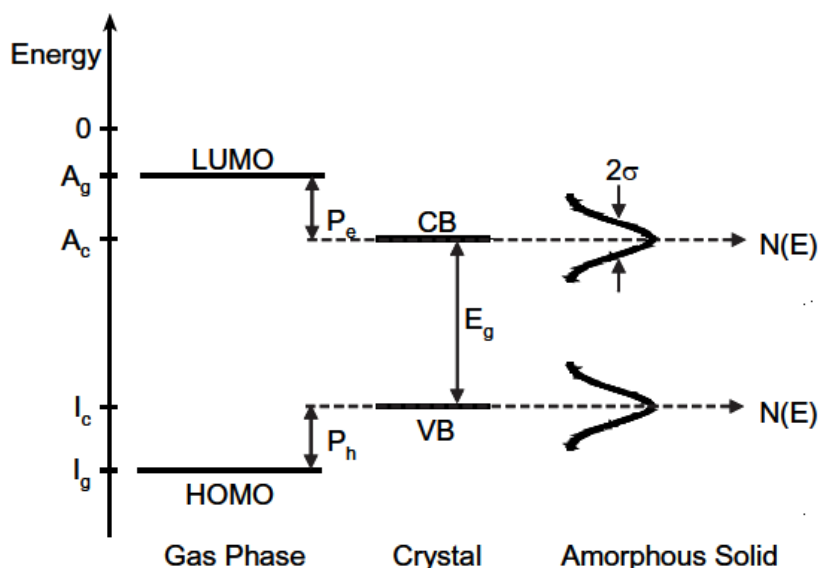


Figure 7. Energy levels of an isolated molecule (left), a molecular crystal (middle) and an amorphous solid (right). [8]

### 3.3.1. n-type Organic Semiconductors

There are considerably fewer molecular structures that have been identified as preferentially electron-carrying (n-channel/type) semiconductors (Figure 8, although the list has grown rapidly in the past two years and now approaches 100 total compounds. n-type OSCs are needed to take advantage of the greater power efficiency of complementary transistor circuits, as well as to develop devices that rely on p-n junctions.

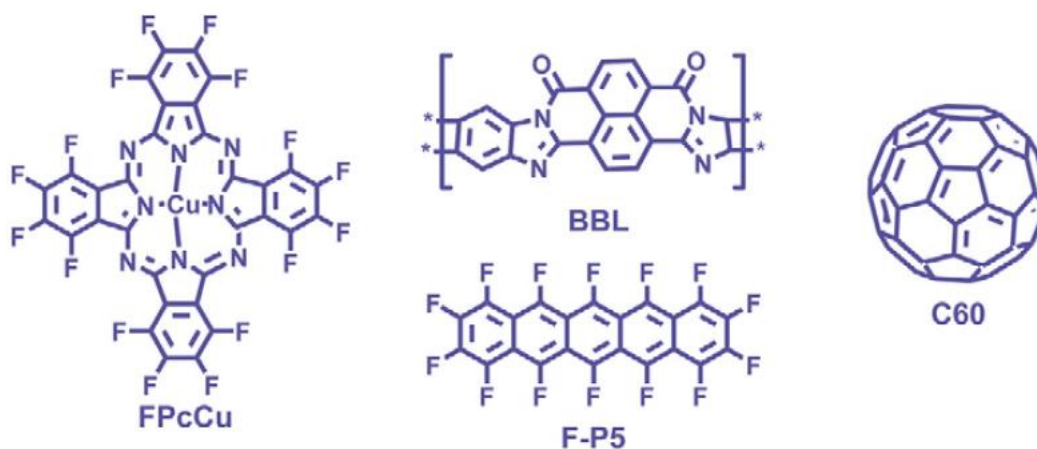


Figure 8. Commonly used n-type organic semiconductors, copper complex FPcCu, BBL (polybenzimidazo-benzoisoquinoline), C60 (Carbon 60 Fullerene), F-P5 (5 ring Fluorinated Pentacene).

$\pi$ -bond frameworks that can be the basis of n-OSCs must provide sufficient stability of injected electrons relative to environmental quenchers such as oxygen and synthesis residues in and around OSCs. For thermodynamic stability of the radical anion to oxygen and water, the reduction potential of an n-type OSC must be more positive than the SCE (standard calomel electrode)[9]. A challenge of using such materials is to prevent their unintentional doping by environmental agents that would render them conductive. The lowest unoccupied molecular orbital (LUMO) energy levels of most conjugated organic compounds lie outside the preferred ranges for electron transport making them unsuitable for devices. The interest in n-type semiconductors is further enhanced by the fact that both n- and p-type materials are necessary if logic circuits based on organic semiconductors are to be realised[10].

### **3.3.2. p-type Organic Semiconductors**

The majority of conductors in a p-type semiconductor are holes. The preference for conduction of holes is determined by the highest occupied molecular orbital (HOMO) energy level.

The main classes of hole-carrying molecular solid OSCs include fused rings (such as pentacene, thienothiophene, benzodithiophene, dithienoanthracene, and tetracene), short oligomeric chains of rings (various combinations of thiophenes, phenylenes, thiazoles, and pyrroles), ethylene and ethynylene groups, and selenophenes. Once again, of all these only a select few have been investigated as diodes[9].

The number of research groups devoting significant effort to the synthesis of OSCs has grown from just a few in the late 1990s to hundreds at the present time[9]. There are now hundreds of compounds that have been demonstrated as hole-transporting (p-type) semiconductors in field-effect transistors (FETs). The majority of diodes investigated involve p-type OSCs, however, the majority of literature focuses on FETs rather than diodes

### **3.3.3. Charge Transfer Complex**

It is well-known that association of a molecule of low ionisation potential (an electron donor, P3HT) with a molecule of relatively high electron affinity (an electron acceptor, O<sub>2</sub>) can lead to a weakly bound donor-acceptor complex or charge transfer complex (CTC). Upon

association, the physical properties of the donor and acceptor are perturbed and new properties arise. P3HT is a  $\pi$ -conjugated polymer which is an intrinsic semiconductor when undoped. The formation of the CTC results in the increase of conductivity but causes a decrease in the mobility[11]. The inverse relationship indicates that the carrier concentration is increasing with oxygen concentration. The conductivity ( $\sigma = \eta e \mu$ ) of the films increases linearly with oxygen pressure. In a vacuum the conductivity is  $4 \times 10^{-8}$  S/cm and  $2 \times 10^{-6}$  S/cm at pressure of one atmosphere. J-V curves are fully reversible upon the removal or addition of oxygen. These changes dramatically affect the electrical properties of Schottky diodes.

### 3.3.4. Poly(3-hexylthiophene-2,5-diyl), (P3HT)

The organic semiconducting polymer used in this project is P3HT a conjugated thiophene polymer. It is very popular for organic semiconductor research due to its high mobility and solubility in a range of organic solvents. The monomer unit of P3HT is shown in Figure 9.

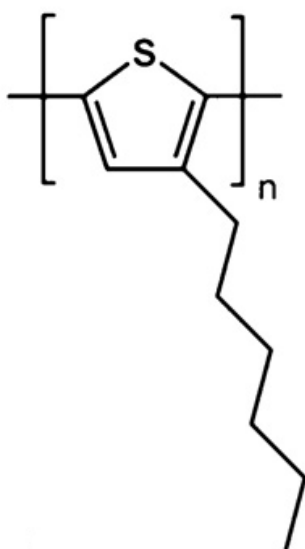


Figure 9. A poly(3-hexylthiophene-2,5-diyl) monomer unit.[12]

#### 3.3.4.1. Regioregularity

A regioregular polymer is composed of the same isomers of the monomers as shown in Figure 10. where a regioregular polymer can be seen on the left with the side chains are facing in the same direction along the chain, polymer that is not regioregular is called

regiorandom. A polymer with a high degree of regioregularity will have a greater degree of crystal packing, and therefore increase charge transport mechanisms.

Head to Tail (HT)

Head to Head (HH)

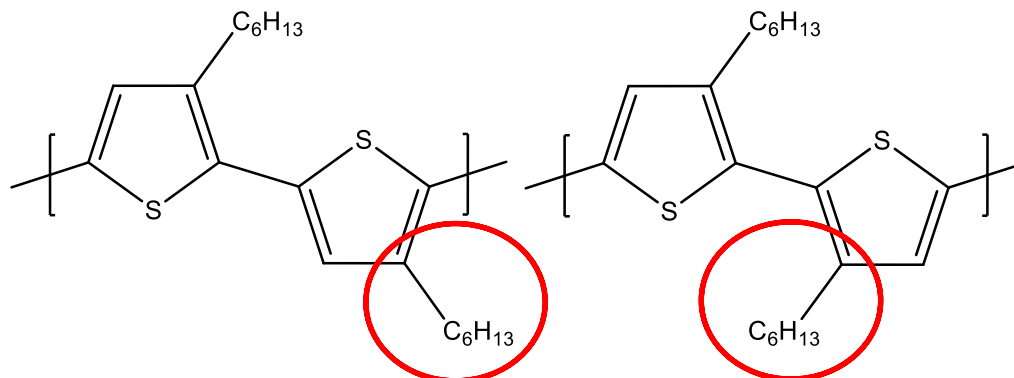


Figure 10. Left, Head to Tail, Regio-regular unit of Poly(3-hexylthiophene-2,5-diyl). Right, Head to Head regio-irregular.

It is often not possible to make a polymer that is 100% regioregular so the value is often quoted on prepared polymer. Electronics grade P3HT is 91-94% regioregular and has a molecular mass of 50-70k Daltons. Despite lower molecular weight polymers forming a more crystalline structure; a large molecular weight has been shown to improve mobility in transistors made with P3HT[13]. The greater mobility is attributed to better interconnectivity within the polymer network.

#### 3.3.4.2. P3HT Crystal Packing

The crystal packing of P3HT relies on a number of fabrication parameters including annealing parameters, solvent annealing and also the regioregularity of the polymer.

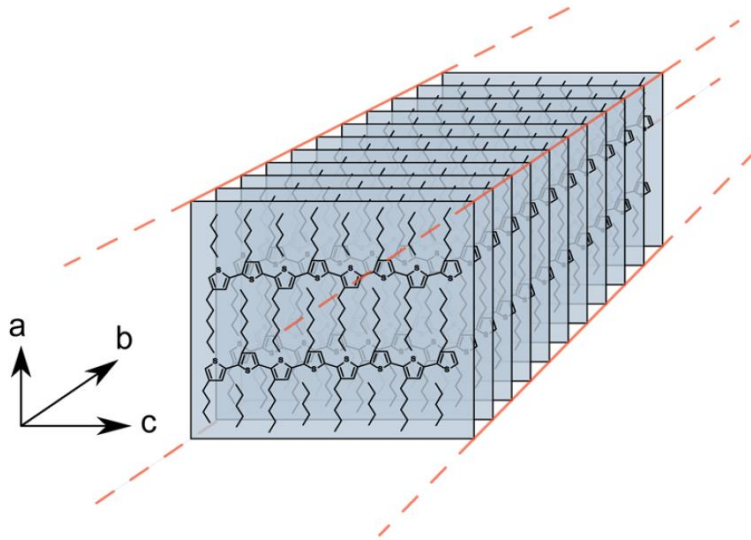


Figure 11. A diagram of the crystal packing of P3HT[14].

The crystallinity of the P3HT layer (Figure 11) highly impacts the electrical properties, it has been reported that solutions of P3HT left to sit for long periods (~months) form fibrils in solution from crystal packing[14]. The mobility and hence the conductivity along the length of the fibrils is twice as much than perpendicularly. [14], [15], [16] When these fibrils are deposited by spin coating they preferentially lie in the horizontal plane, however vertical type diodes conduct perpendicular to the surface so the device performance will suffer.

### 3.4. Organic Diode Characterisation

The electrical characterisation of diodes is different for each type of diode, which is due to the structure of the diode. A Schottky diode's characteristics are due to the Schottky barrier formed between a metal and a semiconductor. In contrast the p-n junction's diode properties are due to the interface between a p-type and an n-type semiconductor. The characterisation of these two types of diodes is different and outlined below.

Characterisation of electrical properties varies greatly from publication to publication. These properties can also be described by Pool-Frenkel emission and tunnelling[17]. Electrical properties can include Schottky barrier height, depletion layer, mobility, capacitance, series and shunt resistance and rectification ratio[18, 19].

#### 3.4.1. Schottky Characterisation

Characterisation of Schottky diodes include J-V (Current-Voltage) curve, capacitance, rectification ratio, ideality, built-in voltage, barrier height, SCLC (Space Charge Limited Current)[20], bulk limited current, mobility, rectified voltage[21]. The depth of electrical characterisation on organic Schottky diodes in the literature to date is inconsistent.

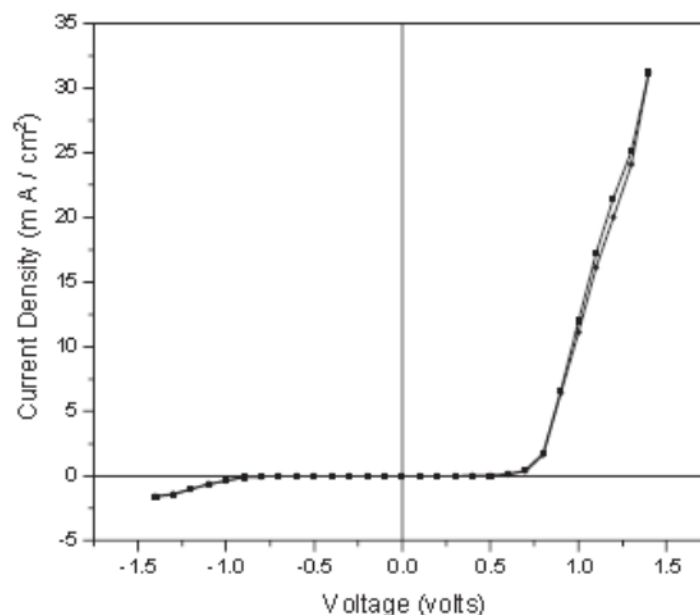


Figure 12. A J-V characteristic curve of PAn-PVC composite - Indium metal junction. [22]

Current-Voltage curves (Figure 12) are the standard method for electrical characterisation of diodes, in which a DC bias voltage is applied across the diode and the corresponding current is measured. The most common voltage range for J-V characteristic curves was +/- 2 V which is enough to characterise the diodes, however, many studies do not include the reverse break-down voltage, which is essential to higher voltage applications.

### 3.4.1.1. Series Resistance

Series resistance ( $R_{\text{Series}}$ ) of a diode is the resistance of the diode in the conducting regime. It is often modelled as a series combination of a diode and a resistor with resistance  $R$  through which the current ( $I$ ) flows [23]. Many methods of modeling series resistance have been developed since the discovery of the solid state semiconductor. Norde [24] developed a model which included the assumption of a perfect diode i.e. ( $n=1$ ) which is definitely not the case for any organic diodes and requires J-V characteristic curves of the same sample at different temperatures. Cheung and Cheung [23] and Sato and Yasumura [25] attempted to improve the analysis by compensating for diodes with high resistance. A simple model called the Piece-Wise-Linear equivalent circuit includes an ideal diode, a resistor and a voltage source (Figure 13).

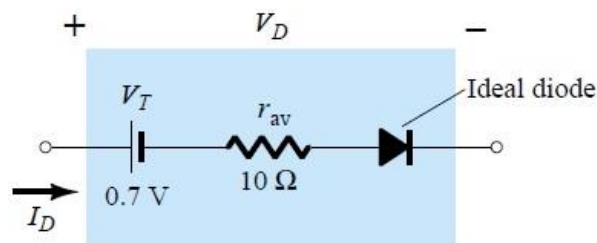


Figure 13. Piece-Wise-Linear Equivalent Circuit

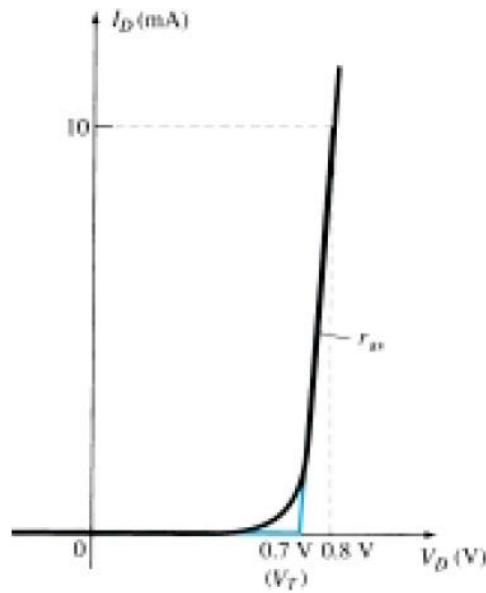


Figure 14. Piece-Wise-Linear equivalent circuit representation of the characteristic curve  
 The voltage source is not an actual source; instead it represents the voltage potential of the depletion region that must be overcome before conduction occurs. The series resistance was calculated from Equation 1 below.

$$r_{av} = \frac{\Delta V}{\Delta I} \Big|_a^b \quad \text{Equation 1}$$

Note that this is the inverse of the slope and is Ohms law applied over a range to increase the accuracy of the result (Figure 14).

### 3.4.1.2. Shunt Resistance

The Shunt Resistance ( $R_{\text{shunt}}$ ) is simply extracted from reverse current of the J-V characteristic curve. The current approximately increases linearly as voltage becomes more negative.  $R_{\text{shunt}}$  can be calculated similarly to  $R_{\text{series}}$  the inverse of the slope of the of J-V characteristic curve according to Ohms law. The resistance could be calculated from a single point but to improve the accuracy the slope is taken across the whole negatively biased region.

### 3.4.1.3. Rectification Ratio

The rectification ratio is a ratio between the forward and reverse current, the ratio is calculated from J-V curves as the ratio of current at + X Volts to the current at -X Volts. There is no standard on what voltage to calculate the rectification ratio and is commonly

chosen to show the maximum rectification. These maximum results can show the capability of the device but don't allow direct comparison between devices at a specific voltage[26].

The switch on voltage can also be extracted from the J-V curve, and is the minimum voltage required to overcome the depletion region of the junction in the forward current direction. Below the built-in voltage the junction will be dominated by insulating properties and will result in an inaccurate rectification ratio[27].

#### 3.4.1.4. Schottky Diode Equation

According to the thermionic emission model[3], the J-V relationship for an inorganic Schottky barrier is given as:

$$J = J_0 \left( \exp\left(\frac{qV}{nkT}\right) - 1 \right) \quad \text{Equation 2}$$

Where  $J_0$  is the saturation current density,  $e$  is electronic charge,  $n$  is the ideality factor,  $k$  is the Boltzmann constant and  $T$  is the absolute temperature. The thermal voltage  $V_T$  is defined as  $\frac{kT}{q}$  and when the bias voltage  $V \gg V_T$  the -1 term in Equation 2 can be ignored and so the above equation reduces to:

$$J = J_0 \exp\left(\frac{qV}{nkT}\right) \quad \text{Equation 3}$$

where  $I$  is the current through the diode,  $V$  is the voltage across the diode,  $I_0$  is the saturation current,  $n$  is the ideality factor and  $T$  is the temperature in Kelvin, and  $q$  and  $k$  are both constants. By taking the log of both sides of the equation gives:

$$\ln(I) = \ln(I_0) + \left(\frac{q}{nkT}\right)V \quad \text{Equation 4}$$

The resultant plot will be linear with the slope equal to  $\left(\frac{q}{nkT}\right)$  and the y-intercept equal to the saturation current  $\ln(I_0)$ . The slope  $\left(\frac{q}{nkT}\right)$  can then be used to calculate the ideality  $n$ . The characterisation was developed for inorganic Schottky diodes but is applied to organic diodes because the same underlying principles of semiconductor theory apply, however this may not be a good measure.

#### 3.4.1.5. Ideality

Ideality is a numerical description of how close the diode resembles an ideal diode from Equation 2 ideality can be calculated from the slope of a log J vs. bias voltage in the linear

region. An ideal diode will have a slope of 1 and as the diode becomes less ideal diode the value will increase. The ideality of a diode is a measure of the amount of charge traps which cause other factors including series resistance, capacitance and recombination. Even though the value is critical for measuring the quality of the diode, it is only occasionally reported.

Deviations in the ideality factor from one indicate that either there are unusual recombination mechanisms taking place or that the recombination is changing in magnitude. Thus the ideality factor is a powerful tool for examining the recombination in a device. For silicon based devices the ideality ranges from 1 to 2, but organic diodes it can range up to 11 due to a greater number of charge traps[28].

There are several factors that can affect the measurement of ideality. At low voltages the shunt resistance ( $R_{shunt}$ ) dominates the diode performance and causes a large peak in ideality, resulting in an inaccurate value, it is usually not possible to correct for the effects of  $R_{shunt}$ . While at high positive voltages ( $V > + 2$  volts) in a J-V curve the series resistance dominates and causes a large peak in the ideality factor curve. The effects of resistance are particularly pronounced in OSC diodes, as  $R_{shunt}$  is quite high ( $\sim M\Omega$ ), and the series resistance is also quite high ( $k\Omega$ ), both of which increase the ideality value of the diode. The calculation of the ideality is then taken from a voltage range between +0.5 Volts and +1V to avoid the effects of the series and shunt resistances.

### 3.5. Organic Diode Applications

Diodes have not received as much attention from the organic electronics community as FETs. However, they have an important role to play in organic-based circuitry. A high rectification diode is quite important for a broad spectrum of electronic applications[29]. Applications include rectification from AC to DC, isolating signals from a source, voltage reference, controlling strength, mixing and detection of signals, light emitting diodes and laser diodes.

Electrical and optical properties of diodes can vary depending on the chemical properties. Diodes are traditionally thought of as non-photo-active electrical components but the band-gaps of organic semiconductor diodes often lie within the energy range of visible light. These diodes can emit or accept light, depending on their band-gaps these diodes can be light emitting diodes, photo-diodes or photo-voltaic cells[30]. It also has been shown by Adachi *et al.* that organic thin films can also support extremely high current densities over  $12000\text{A}/\text{cm}^2$ [31], these properties reinforce the promise of OSCs as potential RFID components. However, RFID requires high frequency rectifying circuits for power supply, high frequency rectification by OSCs has only been achieved with vacuum processed small organic molecules[32, 33]. For OSCs to be a viable option in RFID they must be commercially competitive, this can only be achieved by solution processed polymer circuits.

The majority of research on organic semiconductor diodes has been focused on Schottky diodes. The major limiting factor of organic semiconductors is their poor electron mobility which limits frequency response[34]. Properties of Schottky diodes can compensate for this due to the barrier at the metal-semiconductor interface which allows for fast recovery times.

The majority of organic Schottky diodes use p-type semiconductors and the most researched of these are doped polyaniline, polypyrrole and their composites[22, 35]. A large focus was put on polypyrrole in the 1980's and has been summarised in a review[36]. Composites have also been investigated such as polypyrrole doped with polyethylene oxide[37]. Even Methyl-red a common indicator dye that turns red in acidic solutions but has also been fabricated into a Schottky diode[38]. The primary solution processed devices are based on poly(3,4-ethylenedioxythiophene) due to its solubility in many organic solvents and electrical properties.[14, 39, 40].

A potential application for OSC Schottky diodes lies in their use as a rectifying circuit for the incoming RFID signal. Printable diodes are lower cost and possibly flexible, which are both

advantages for RFID tags. The operating frequency can range from 123 kHz to 5.8 GHz depending on the class of the tag. This is a large range and the lower end is still quite demanding for OSC. At high frequencies capacitance effects must be minimised to allow the circuit to function[41].

To date different production methods of OSC layers have been investigated including electro-polymerisation in solution, spin coating and vacuum deposition. The vast majority of publications on Schottky diodes focus on the vacuum deposition of the organic semiconducting layer [19, 38, 42-44]. The advantage gained from vacuum deposition is higher crystal ordering of the deposited OSC, improving the electrical properties. A high frequency diode operating at 13.56Mhz[41] on a flexible substrate has been reported and a 50 MHz rectifier based on an organic diode set a new standard, but both must be fabricated by vacuum evaporation[45]. This research demonstrates that OSC electrical devices can operate in high frequency applications. However, the limitation of expensive production limits the commercial viability of the devices

### **3.5.1. Solution Processed Diodes**

In order to develop low cost, large area polymer electronic market opportunities (particularly device fabrication on flexible substrates) solution-processable conjugated polymer development was primarily aimed at spin- and dip- coat processing, which are typically lower cost options for processing organic electronics[46]. Soluble polymers can be used in printing techniques such as ink-jet printing, roll to roll processes which include rotogravure and offset printing. The advantages afforded by printed circuits go beyond cost reduction to include other advantageous properties such as increased flexibility and durability.

Some air stable pentacene rectifying circuits have been developed on flexible substrates but were produced with wet etching techniques and have been based on transistors[47]. Important factors in the optimisation of this include the reduction of diode area, improving Ohmic contact and the hole mobility and thickness of the semiconductor layer[48]. A series of solution processed Schottky diodes with good rectification were fabricated, but severe decay over 3 months was observed, which highlights air stability as a barrier to producing low-cost, low-performance diodes[39].

A major issue with OSC diodes is conduction in the OSC, the conduction or mobility of these OSCs are at most one tenth that of amorphous silicon. Despite this drawback, an example of a Gravure printed diode exists showing excellent promise for this technology.

In a metal-semiconductor junction, a metal contact with a work function less than the p-type semiconductor will form a Schottky barrier, if the metal's work function is equal to or greater than the p-type semiconductor the contact will be Ohmic, the opposite is true for n-type semiconductors[4]. As a p-type semiconductor, P3HT has a function of 4.7 and apart from gold, all of the metals in Table 1 have a work function lower than P3HT and hence will form rectifying contacts. Gold has a higher work function than P3HT and will form an Ohmic contact.

Metal	Work function (eV)
Titanium	4.09
Indium	4.12
Aluminium	4.28
Tin	4.42
Gold	5.1

Table 1. Work functions of metals commonly used in organic diodes.[44]

Chang, Sun [49] et.al. demonstrated that drying time increased mobility in thin film transistors. They found that low boiling point solvents such as chloroform (~61°C) and xylene (~137°C) which dried within seconds of spin coating, resulted in lower mobilities of 0.012 and 0.024 cm<sup>2</sup>/(V.s) respectively. However 1,2,4-trichlorobenzene with a boiling point of 214.4°C, dried over a 5-10 minute range resulted in the highest mobility of 0.12 cm<sup>2</sup>/(V.s). 1,2 - dichlorobenzene was selected for this project for its high boiling point (180.5 °C) which allows for slow evaporation but also a lower boiling point to remove solvent completely during annealing.

## **Project Aims**

The aim of this thesis was to investigate the relationship between the fabrication parameters of a model polymer diode system and its electrical properties.

The fabrication parameters investigated are:

- Drying time between spin-coating the polymer layer and annealing the solution.
- Temperature at which the diodes are annealed.
- Amount of time the diodes annealed.
- The thickness of the polymer layer which is dependent on:
  - The concentration of the polymer solution.
  - Spin speed of during deposition.
  - Length of deposition time.
- Fabrication of devices in Air.
- Fabrication of devices in an inert environment.

The critical electrical properties measured and calculated were:

- Series resistance.
- Shunt resistance.
- Rectification ratio.
- Ideality.
- Testing in of devices in air and inert environments.

In addition to the investigatory aims of this project; organic diodes were fabricated for comparison with an inorganic diode:

- To compare rectification ratio.
- Create a half-wave rectification circuit including inorganic electronic components to rectify alternating current to direct current.

# 4. Experimental

## 4.1. Fabrication

The project is based around the fabrication parameters of a model organic diode. A standardised and reproducible fabrication method was developed. To examine the effect of each fabrication parameter on the electrical properties, one fabrication parameter was varied while the rest of the parameters were controlled.

### 4.1.1. Fabrication Parameters of Devices

The fabrication parameters outlined in the project aims were systematically varied to discover their effect on the electrical properties. The parameters below are defined in an idealised diagram below (Figure 15).

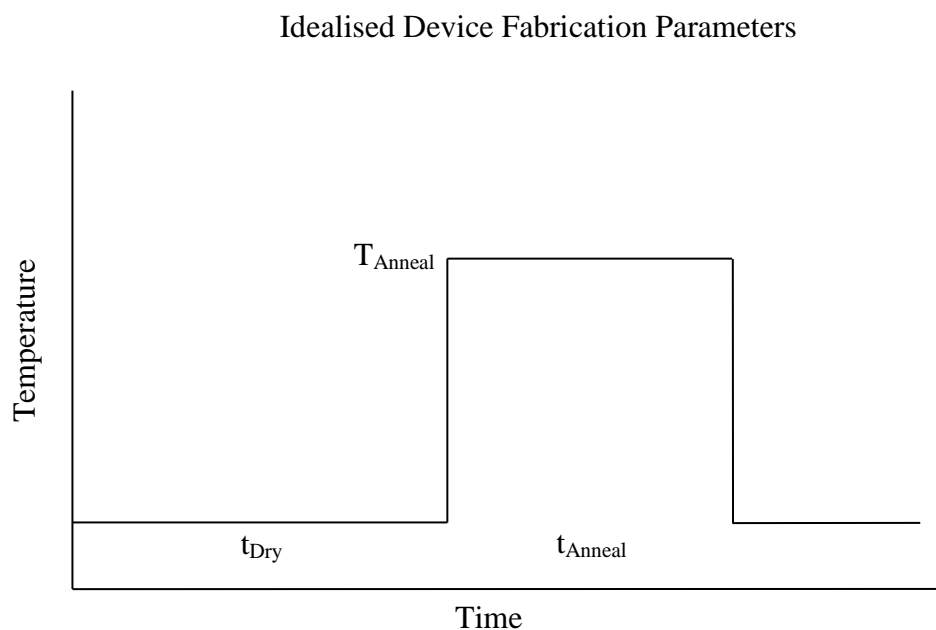


Figure 15. An idealised device fabrication parameter diagram, where  $T_{\text{Anneal}}$  is the temperature at which the device is annealed,  $t_{\text{Dry}}$  is the time between spin-coating and annealing and  $t_{\text{Anneal}}$  is the amount of time the device is annealed.

### 4.1.2. Device Fabrication Recipe

A generalised fabrication recipe was developed for consistent fabrication of devices. The recipe below is for devices fabricated in the glove box, for devices fabricated in air the P3HT solution the steps in section 1 were prepared in a clean laboratory fume hood.

#### 1. Prepare P3HT solution 24hrs before use.

##### Outside Glove box

1. Clean glass bottle (water, ethanol rinses, N<sub>2</sub> dry)
2. Weigh out solid P3HT to 3% = 30mg/ml
3. Put the cap loosely on the bottle
4. Take the bottle into the Glove box

##### Inside the Glove box

1. Syringe DCB from bottle through a 0.45 micron filter (to remove large particles) in the Glove box (2 piece syringe).
2. Remove filter and syringe x ml of DCB into the bottle.
3. Add mini stirrer bar.
4. Place lid on tight.
5. Put the solution on to stir ~300 rpm at 60deg for at least 12 hours.

#### 2. Prepare Glass slide and Bottom Contact

1. Cut a microscope slide into a square ~1"x1"
2. Record a serial number on the slide
3. Sonicate the slide in DI water for 10 mins
4. Rinse with ethanol and immediately dry with N<sub>2</sub>
5. Immediately place in sample container face down (serial number side up)
6. Take the samples into the Glove box

#### 3. Evaporate Bottom Contacts

1. Insert sample holder onto chuck
2. Place samples in sample holder with serial number down
3. Place mask and attach with screws
4. Run evaporation cycle Ti 5nm then Au 30nm
5. Remove samples from chuck and place in containers

#### 4. Spin coat P3HT

1. Prepare hotplate for spin-coating by pre-setting it to the annealing temp 130deg
2. Prepare bench for spin coating by having clean sample holders, tweezers and micro-pipette readily available
3. Select spin pattern recipe on the spin coater
  - a. #11 For thinnest organic layer (500rpm for 10s, 2000rpm for 30s)
  - b. #10 For thinner organic layer (500rpm for 10s, 1000rpm for 30s)
  - c. #9 For thicker organic layer (500rpm for 30s)
4. Place sample centrally onto the chuck and turn on vacuum
5. Deposit 20 microliters of solution evenly on the substrate and press start

6. Remove sample and place to aside to dry, enclosed in a wafer container or on hotplate to anneal
  - a. Place sample in holder and cover for 5 minutes then place on hotplate for 20mins

#### 5. Evaporate Top Contacts

1. Place sample in sample holder and ensure the orientation is correct ( $90^0$  or  $180^0$  to contacts)
2. Run evaporation cycle of Aluminium 30nm
3. Remove samples from chuck and place in holders.

The cleanliness during fabrication is of the utmost importance. The thin films of the polymers and metals involved are of the range 10nm to  $1\mu\text{m}$ . A “speck” of dust can range from 2.5 to  $10\mu\text{m}$  if this dust adheres to the surface at any stage of the process will be thick enough to cause imperfections through multiple layers resulting in electrical shorting or insulating devices rendering them resistive or non-conductive respectively.

### 4.1.3. Device Fabrication in Air

A clean room facility was not initially available for the project. Devices fabricated in atmospheric air were fabricated in a laminar flow hood where practical. 1,2-dichlorobenzene was used for all spin coating solutions because it has a boiling point of  $180.5\text{ }^\circ\text{C}$  which has a slow evaporation compared to solvents commonly used and in turn provides a longer time period to investigate morphology changes. All spin coating solutions were used within a week of preparation to avoid the formation of polymer fibrils[14]. A pre-spin of the solvent was undertaken to ensure that any dust was removed. An added bonus to the pre-spin was that the wetting of the polymer solution to the substrate improved resulting in more homogenous layers.

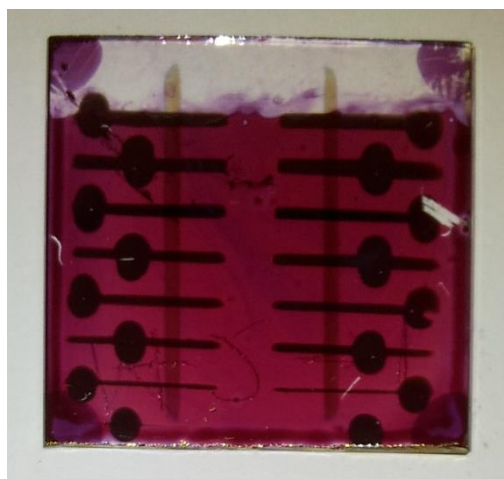


Figure 16. An example of a device produced in Air through sequential deposition of semiconducting polymer and metal electrodes.

Metal layers for devices produced in air were sputtered in a Quorumtech K757X Sputter coater. Two vertical bars are the common gold electrodes were evaporated through a brass shadow mask with two slots cut into it. The purple is annealed P3HT and the darker dots with lines crossing the gold electrodes are the Aluminium electrodes, which was selected for its workfunction (4.28 eV) to create a Schottky barrier. The shadow mask was designed with various widths that intersect the gold electrodes to vary the area of the diodes. As can be seen in Figure 16 each device has 14 diodes at the intersections of the electrodes. The electrodes were designed to keep the diodes electrically isolated but using a common electrode to streamline the testing procedure. The oval shapes on each electrode act as the contact patch for ease of connection to the testing equipment (Figure 16).

#### **4.1.4. Device Fabrication in Inert Atmosphere**

A glove-box was used for fabricating devices in an inert environment atmosphere. The glove-box was equipped with a filtration system, in which dust would be removed via constant circulation through two filters. The glove-box maintained levels of less than 1 ppm of oxygen and water, during experiments (Figure 17).



Figure 17. Innovative Technology Glove-Box commissioned by Angstrom Engineering.



Figure 18. An example of a device fabricated and encapsulated in the glove box. The design is very similar to the devices fabricated in air. The two vertical bars are the common gold electrodes. The purple is annealed P3HT and the silver lines intersecting the gold electrodes are the Aluminium electrodes. The rectangle at the end of the electrodes is the contact patch. The intersection of the gold and Aluminium electrode is the diode area. Each device has 12 diodes on it. The evaporation mask allowed for greater control of the shape, so

the design in Figure 18 has 3 different area sizes with four (4) lots of each to test reproducibility within a sample (Figure 18).

#### **4.1.5. Metal Electrode Evaporation**

During the project a glove-box was commissioned with built in thermal evaporator. Hence the metal layers of devices produced in inert atmosphere were produced by PVD by thermal evaporation in a vacuum chamber controlled by a Covap II SQC-300 commissioned by Angstrom Engineering as seen in Figure 17. The thermal evaporator built into the glove-box also prevented exposure of the devices to atmosphere (oxygen, dust and water) during fabrication.

## **4.2. Electrical Characterisation**

A standard method was developed to mitigate the effects of air exposure while testing. Each diode was tested five times; the first characteristic curve often had a high reverse current, so the second to the fifth characteristic curves were used for the data and averaged to reduce any variation.

The primary method of characterisation is the current – voltage (J-V) characteristic curve. A Keithley 2400 Source Meter ® was used to collect J-V data for the experiments. The source meter's compliance and sweep range settings were tested to understand they would impact the results.

The compliance is an important setting for the source meter which defines the upper-limit of the current range and in turn the resolution of the current. Compliance was set in orders of magnitude ranging from 1A to  $1 \times 10^{-6}$ A. The Keithley has a resolution of 5 ½ digits with 0.012% error[50].

When a characterisation curve is recorded the bias voltage is taken from one extreme of the scale i.e. -4V and stepped at equal intervals to the opposite end of the scale i.e. +4V. A Hewlett-Packard Infinium (500Mhz, 2 GSamples/s) oscilloscope was attached with a 1 MΩ shunt resistance to inspect the process. The bias voltage was zero (0) Volts before and after every sweep. The sweep involves 50 equally wide steps from Start Voltage to Stop Voltage. A double sweep will go from Start V to Stop voltage, jump back to Start V and step up/down to Stop V again.

Despite the sweep being equivalent in both directions, a difference in J-V curves was observed. The current appeared to spike at the beginning of any sweep. Open circuit sweeps were taken for each compliance, voltage range and sweep direction combination as a baseline. For each set of data the associated baseline was subtracted to remove the current spike.

To avoid parasitic capacitance, a voltage sweep rate of less than 0.25 V/s was used to minimise any capacitance effects of the diodes.

The electrical breakdown of a diode occurs when the reverse bias voltage is large enough that the diode begins to conduct on the order of forward current. Silicon diodes can often recover from operating in the breakdown region, however organic diodes do not recover once the breakdown voltage is passed. Conductive paths with graphitic-like structures are formed due to the change of the chemical structure of the carbon chains. Kang et. al. observed reverse breakdown currents of 5 Volts to 24 Volts for organic devices that were 28 nm to ~100 nm thick, respectively[51]. A common non-conductive polymer PTFE has a breakdown voltage of  $19.7 \text{ MV/m} = 0.0197 \text{ V/nm}$  [52]. Considering the thickness of most of the diodes produced was ~100nm then the breakdown voltage would equate to 1.97 Volts. Kang et. al. results were 2.5 times higher, the higher breakdown voltage may be due to the semiconductor material compared to an insulating material. The sweep range of  $\pm 4$  Volts was selected for diodes fabricated in this project as it will not result in breakdown.

## 5. Results and Discussion

The impact of fabrication parameters on the electrical performance of planar gold- poly(3-hexylthiophene-2,5-diyl) – aluminium diodes were investigated. Electrical characterisation of this model system elucidated a strong dependence of diode electrical performance on the majority of the fabrication parameters.

### ***5.1. Equivalent Circuit Simulation and Electrical Characterisation***

An equivalent circuit was determined to understand the electrical properties of the device. Multisim version 11.0 was used to produce the equivalent circuit simulations; it is a graphic user interface that is based on the program Simulation Program with Integrated Circuit Emphasis, which is the standard for electrical circuit simulation.

Power circuits for RFID are commonly on the IC chip but in the case that they are separate the diodes used are high-speed switching diode. An ideal diode block unit was used to simulate the diode. The primary two factors that determine diode performance are the series and shunt resistance.

#### **5.1.1. Equivalent Circuit Simulation**

J-V characteristic curves provide information of the electric properties of a diode. The rectification, forward and reverse currents were used to determine the equivalent circuit based on experimental device performance. The resistances were simulated by the equivalent circuit in Figure 19. V1 is the DC voltage source selected to imitate experiments. R1 is the series resistance and R2 is shunt resistance and D1 is the ideal diode model block. The DC analysis portion of the software was used to simulate the diodes, involving a voltage sweep from -4V to 4V. Capacitances will exist within the diodes but will not be detected by DC analysis with a slow scan rate.

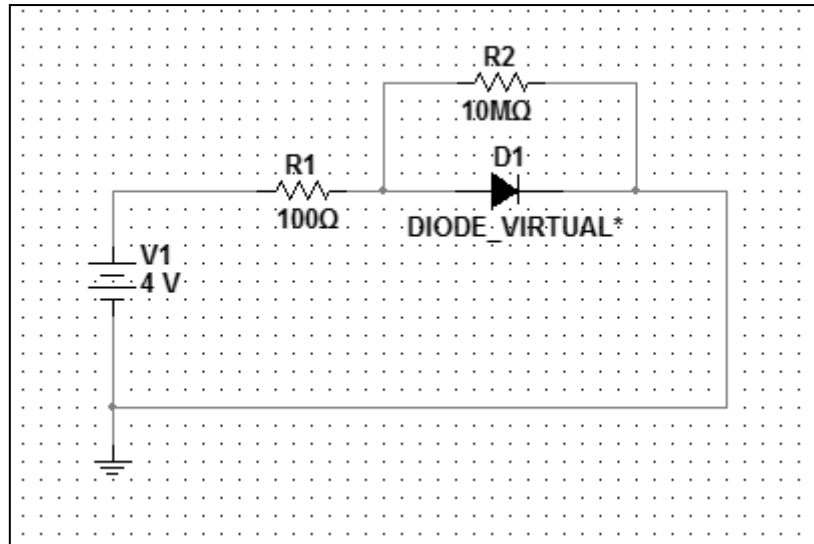


Figure 19. Multisim series and shunt resistance modelling circuit diagram.

### 5.1.2. Impact of Series (R1) and Shunt (R2) resistance

By varying the value of R1 in Figure 19 and holding R2 constant at 10Meg  $\Omega$ , the effects of series resistance can be seen in Figure 20. As R1 is increased, the forward current decreases, with no impact on the reverse current.

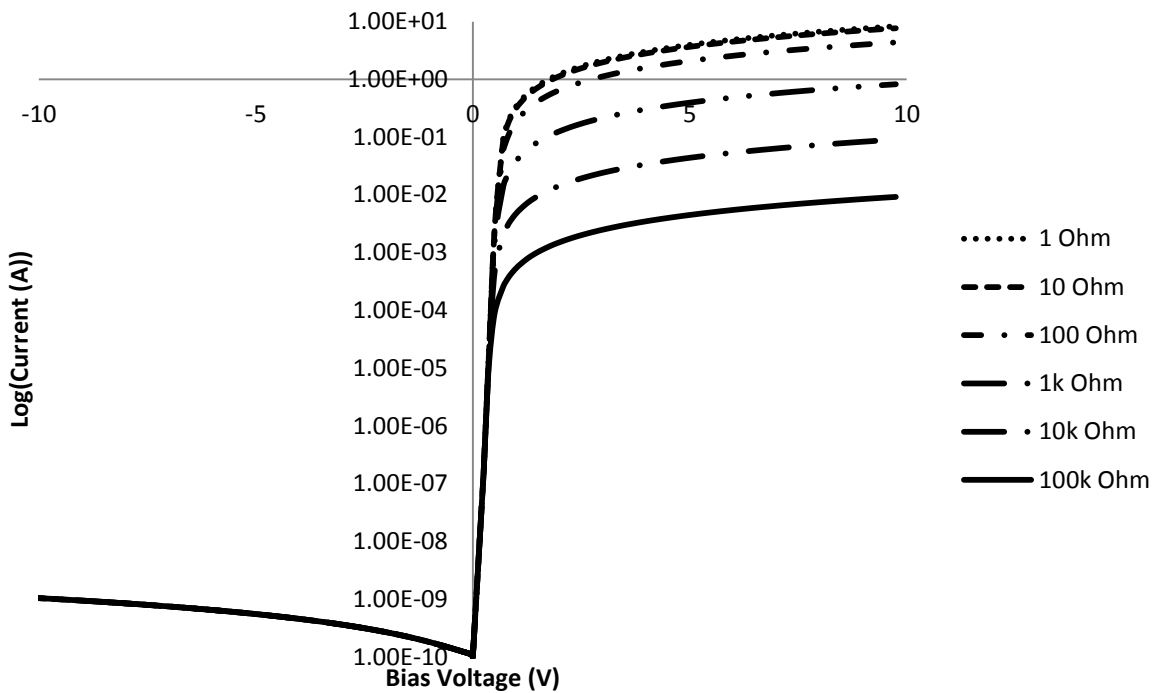


Figure 20. Simulation of Diode Current versus Voltage for a range of series resistors.

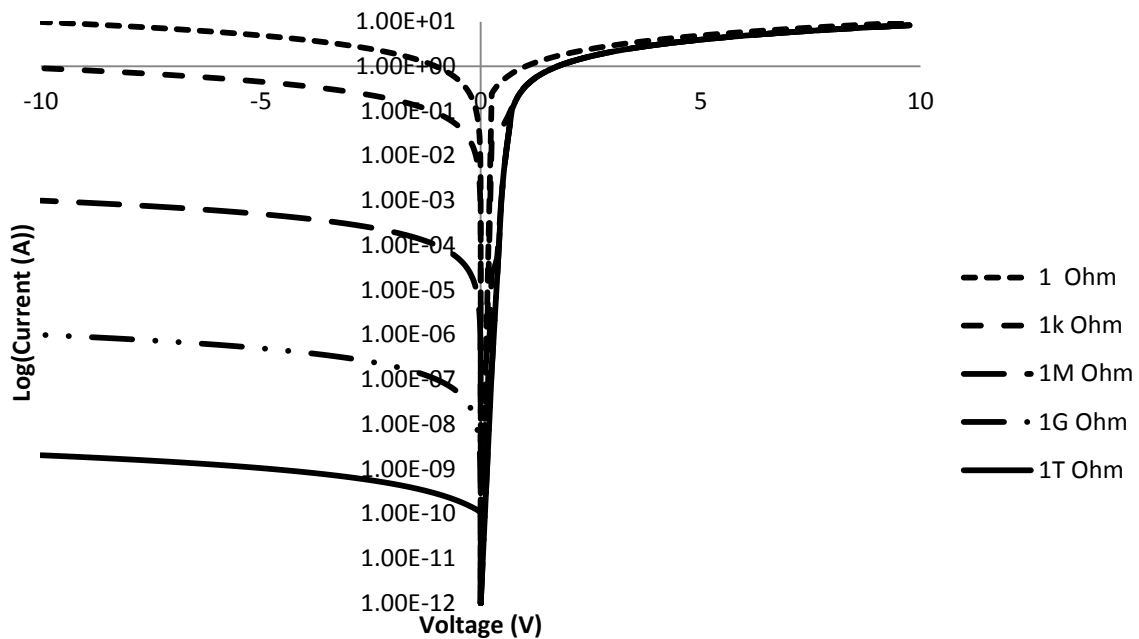


Figure 21. Simulation of Diode Current versus Voltage for a range of shunt resistors. As the shunt resistance is varied with the series resistance held at  $100\ \Omega$ , the reverse bias current decreases as shown in Figure 21. The higher shunt resistance increases the ratio between forward and reverse bias currents, resulting in greater rectification ratios. At very low values of shunt resistance, the current is similar under forward and reverse bias, and therefore the rectification ratio will be low. Increasing the value of  $R_2$  results in the decrease in reverse current and therefore high rectification ratios. The slope of the forward current at low voltages (less than +2 volts) is also decreased.

### 5.1.3. Open Circuit Sweep Test of Kiethley 2400

The Keithley 2400 was tested by leaving the electrical leads intact but no device under test was connected, a voltage sweep of the open circuit was performed and the J-V characteristic was recorded (Figure 22). A non-zero current was recorded, and the values depended on the compliance setting and voltage range. The non-zero current is due to the detection limits of the Kiethley 2400 which is dependent on impedance of the measurement circuit. The Kiethley 2400 has a compliance limit setting which is altered to select an appropriate detection range [53].

### Open Circuit: -4V to +4V Scan with $1 \times 10^{-02}$ Compliance

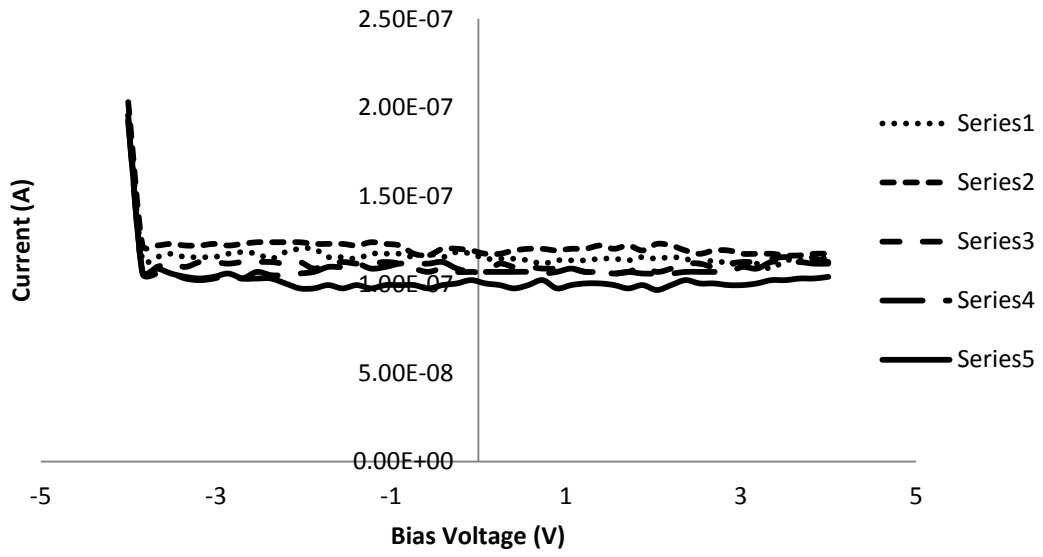


Figure 22. Open circuit voltage scan on Kiethley 2400.

### 5.1.4. Device Testing Protocol Development

It was observed that the initial voltage sweep for the J-V characteristic curve would result in an J-V curve with the greatest forward and reverse current as shown in Figure 23. Since the decrease in the reverse current is relatively greater than the decrease in the forward current, the rectification ratio improves (Figure 23).

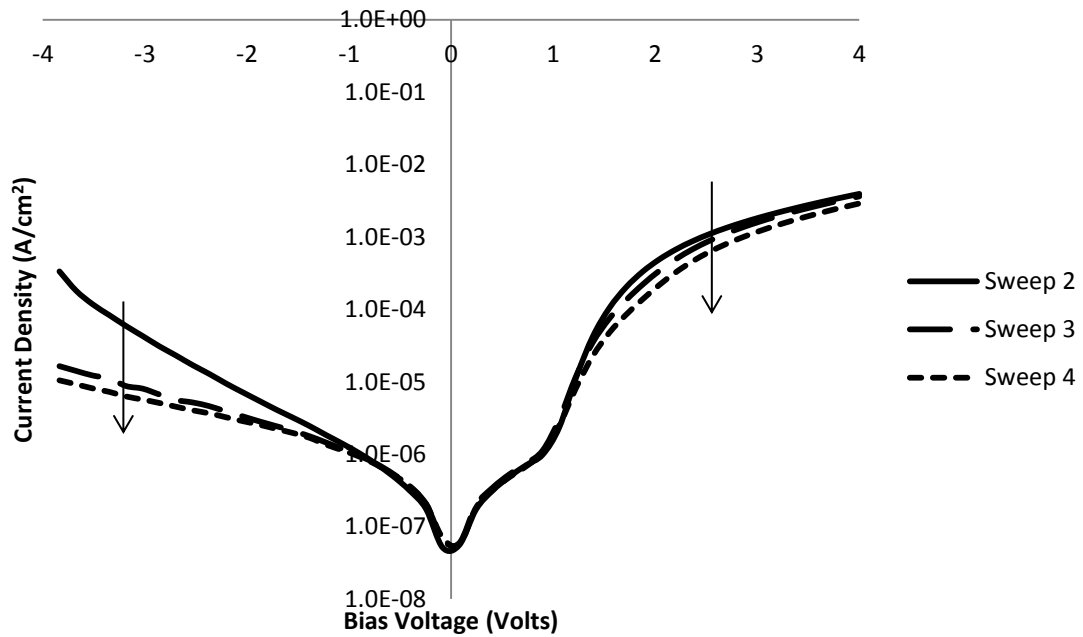


Figure 23. J-V evolution with successive tests.

These results indicate that the application of electrical current affects the electrical properties of the diodes. A diode was tested with a voltage sweep of  $\pm 1$ , 3 and 7 Volts to confirm the voltage did not alter the characteristic curve.

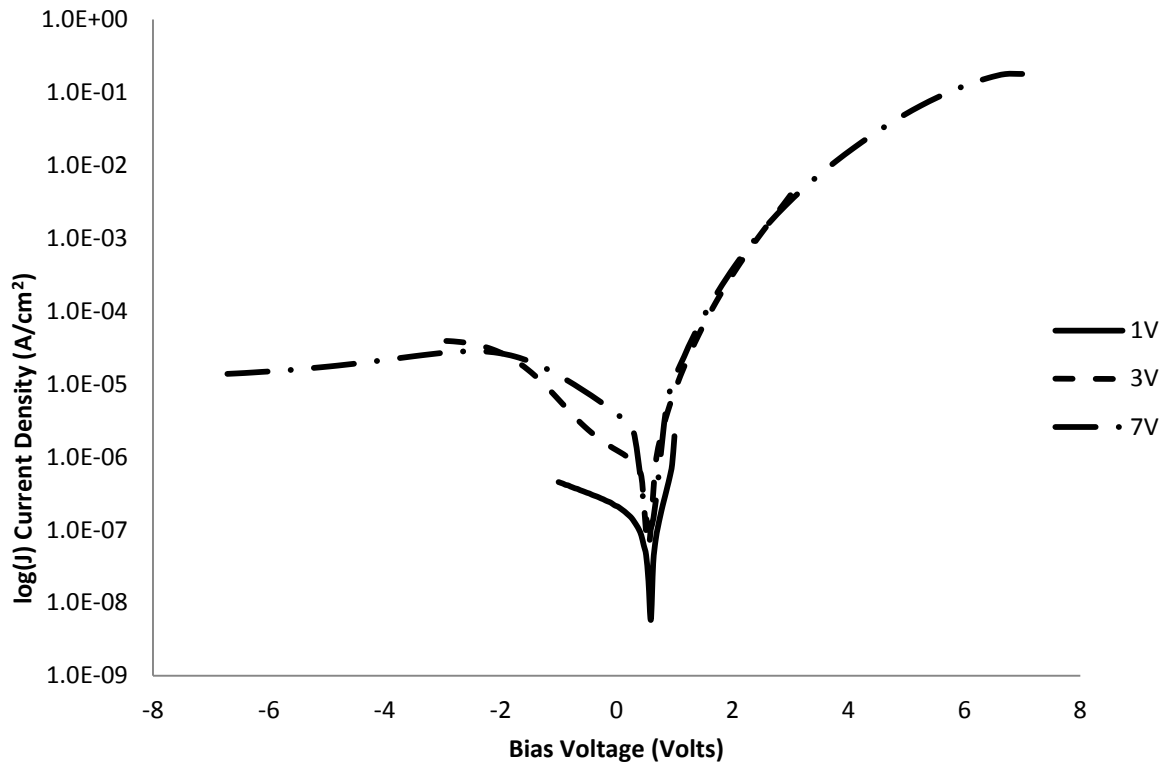


Figure 24. Diode tested under voltage ranges of  $\pm 1$  volt,  $\pm 3$  volts and  $\pm 7$  volts.

As can be seen in Figure 24, the forward currents were very similar for each of the voltage ranges; however the reverse bias current was greater for sweep voltages of  $\pm 3$  volts and  $\pm 7$  volts compared to  $\pm 1$  volt.

Devices tested in air were affected by the surrounding environment (oxygen and water); to account for this phenomenon a standard testing procedure was developed. The first curve would often result in a large reverse current in the characteristic curve, but subsequent curves were more consistent and were therefore used to calculate device parameters. Four subsequent J-V curves were taken and then averaged. Calculations for each of the electrical properties were then made using the Schottky diode model. Devices tested in controlled environments such as encapsulation and inert conditions were investigated later.

### 5.1.5. Photodiode Properties of P3HT Diodes

Exposure of the device to ambient lighting resulted in a significantly higher forward current under the same test conditions, indicating that the Au/P3HT/Al diode behaved as a photodiode. This effect was shown to be fully reversible when tested in dark conditions.

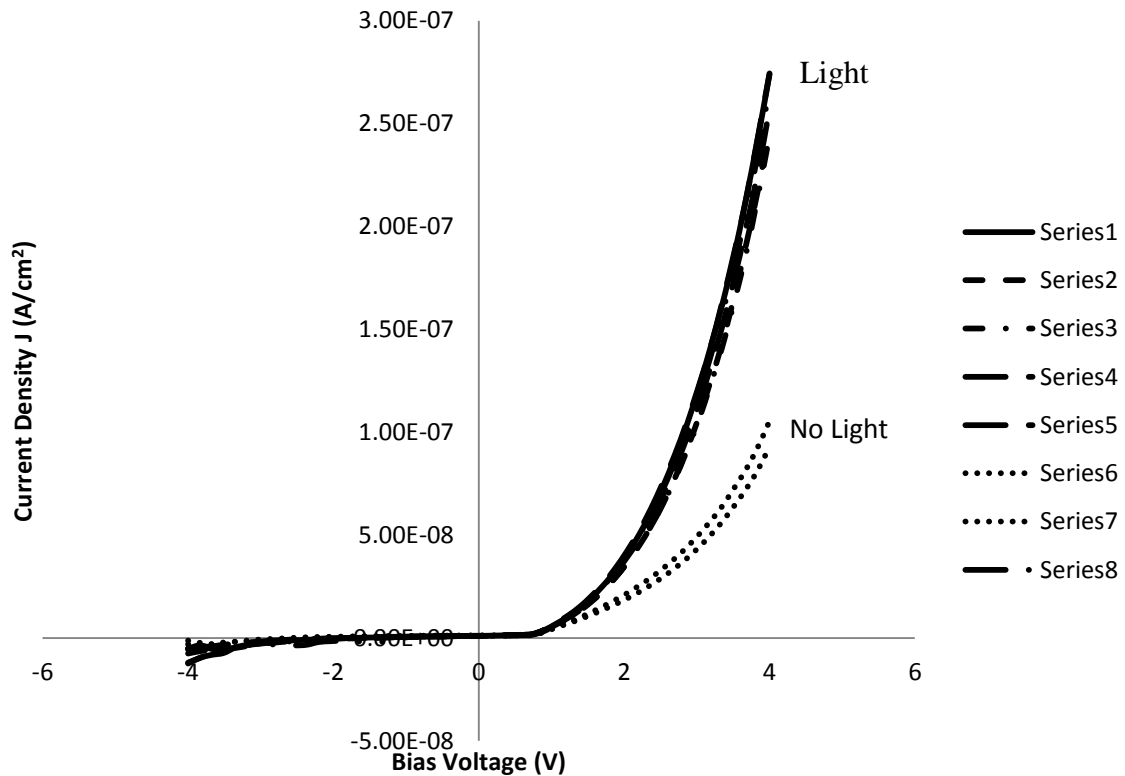


Figure 25. Photodiode properties of Au/P3HT/Al diodes.

The photodiode effect has been observed for P3HT/Al junctions previously [54],[55],[56]. As a result all devices for the entire project were tested in the dark to prevent photocurrent interfering with diode properties and overall results.

The device above was encapsulated and swept in sequential order shown in Figure 25 from series (bias sweep) 1-8. Sweeps 1-5 were taken when the room lighting is on, sweeps 6 and 7 were taken with the lights off, as can be seen the forward current is significantly lower for sweeps 6 and 7 but return to the previous current for sweep 8.

The photodiode effect was confirmed for the diode structure being produced in this project. Data from Figure 25 clearly shows that light has a profound effect on the electrical properties of the diodes. Forward current has clearly doubled when exposed to ambient light therefore photodiode effect was accounted for by electrical testing all subsequent devices in the dark.

## ***5.2. Electrical Parameters of Diodes in Ambient, Inert and Controlled Environments***

### **5.2.1. Fabrication of Devices in Ambient Air**

The device fabrication parameters play an important role in determining the electrical properties of organic diodes. Figure 15 is an idealised device fabrication diagram in which a device is spin coated at time zero. The device was subjected to a controlled range of temperatures and times. The drying time ( $t_{\text{Drying}}$ ) was defined as the time between spin casting the solution and placing the sample on the hot plate to be annealed. ( $t_{\text{Anneal}}$ ) is the amount of the time the sample was annealed at the temperature ( $T_{\text{Anneal}}$ ). The diagram is idealised in the sense that the sample temperature will not instantaneously change from spin temperature (room temperature) to annealing temperature which was between 70°C and 150°C. A large aluminium block was used on the heat source to providing a reservoir of heat which would have reduced the deviation from the idealised fabrication diagram. Devices did not cool from annealing temperature to room temperature instantaneously; this was considered to not be an issue because the samples were left to cool under reproducible conditions each time.

#### **5.2.1.1. Drying Time**

Drying time is an important fabrication parameter because a slower solvent evaporation speed facilitates the growth of a highly crystalline film, inter-chain interactions become stronger and thus improve the electrical properties significantly[49]. 1,2 - dichlorobenzene was selected for this project for its high boiling point (180.5°C) which will dry slowly and can be removed completely during annealing. Drying time ( $t_{\text{Drying}}$ ) was defined to be the amount of time the device was left in the sample holder before it was placed on the hotplate for annealing. Three devices were made with 0, 6 and 10 mins of drying time. Each sample was annealed for 20 mins at 90°C. The variation in the time would arise from handling the samples. One sample was made at a time and after much practice it would be safe to accept a variance of +/- 10 sec. The devices were tested in Air under the same conditions, five cycles were taken and the average of the last four was used for the data analysis.

## Series Resistance

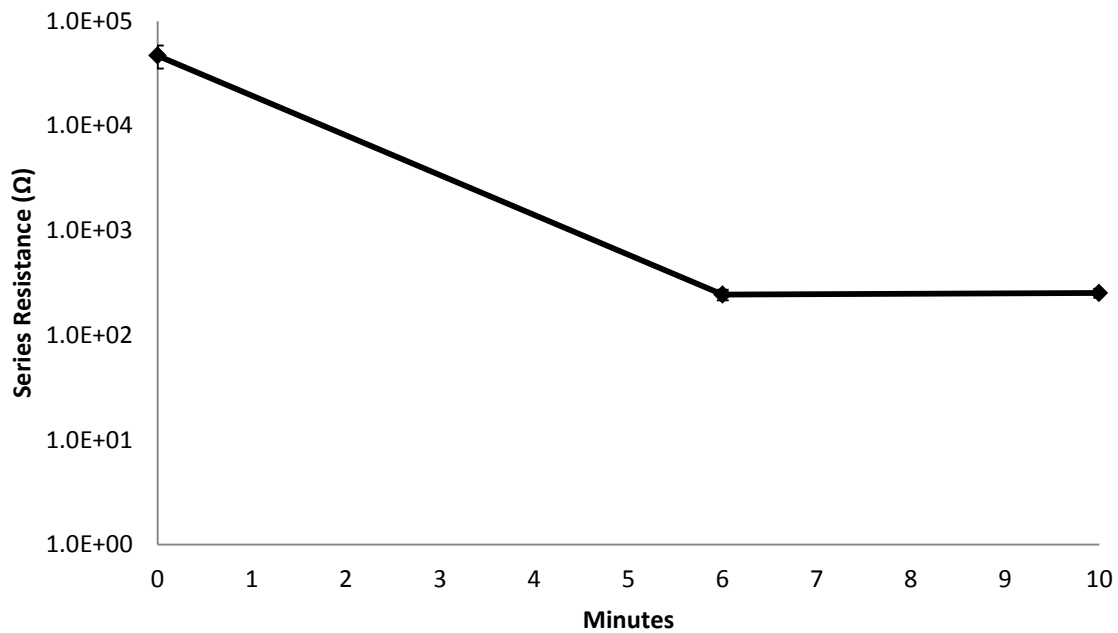


Figure 26. Series Resistance Vs. Drying Time.

Taking the result that the forward current is almost exclusively impacted by the series resistance; it was found that the series resistance decreased by three (3) orders of magnitude as drying time was increased between zero (0) minutes and six (6) minutes (Figure 26). Series resistance appears to plateau after six minutes resulting in diminishing returns with greater drying times. Longer drying times result in a slower evaporation speed facilitating the growth of a more crystalline film with stronger inter-chain interactions, which improves the conductivity and hence results in reduction of series resistance. The decreased series resistance will be beneficial to the diodes overall electrical properties because of greater conduction when the diode is forward biased.

Reduction in series resistance by three (3) orders of magnitude by allowing the sample to dry for six (6) minutes is a great improvement over no drying time; for following experiments a standard drying time was chosen to be five (5) minutes.

## Shunt Resistance

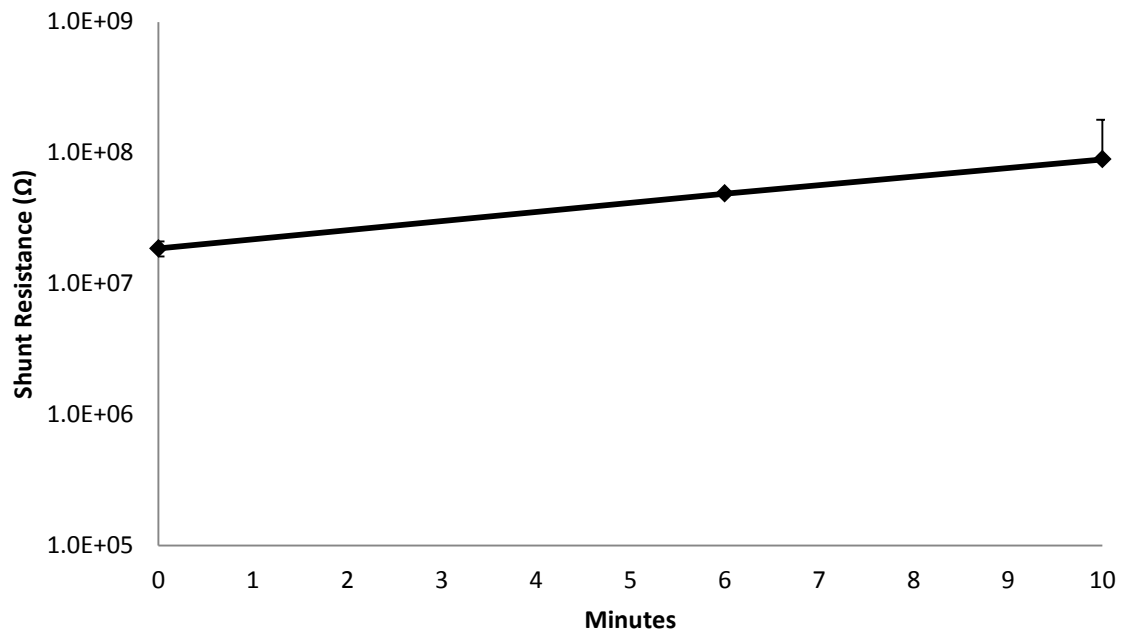


Figure 27. Shunt Resistance vs. Drying Time.

Shunt resistance increased over one order of magnitude over the 0 to 10 minute range, from 18.6 MΩ at 0 minutes to 89.3 MΩ at 10 minutes as shown in Figure 27. A greater drying time results in a larger shunt resistance, improving diode performance particularly the rectification ratio.

## Rectification Ratio

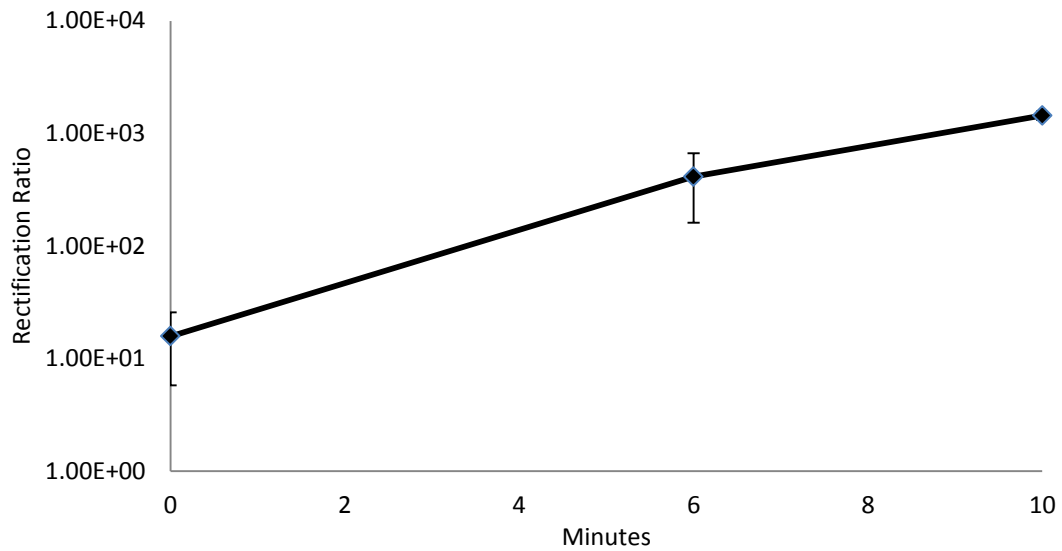


Figure 28. Rectification Ratio versus Drying Time.

The rectification ratio can be seen to increase as the drying time is increased in Figure 28. The drying time massively improved the rectification ratio from a barely rectifying device 15:1 to three orders larger 1440:1. The improvement therefore shows great potential of the diodes as an applicable device by controlling drying time as a fabrication parameter. The rectification ratio increased due to the massive decrease in series resistance and a small change in the shunt resistance.

## Ideality

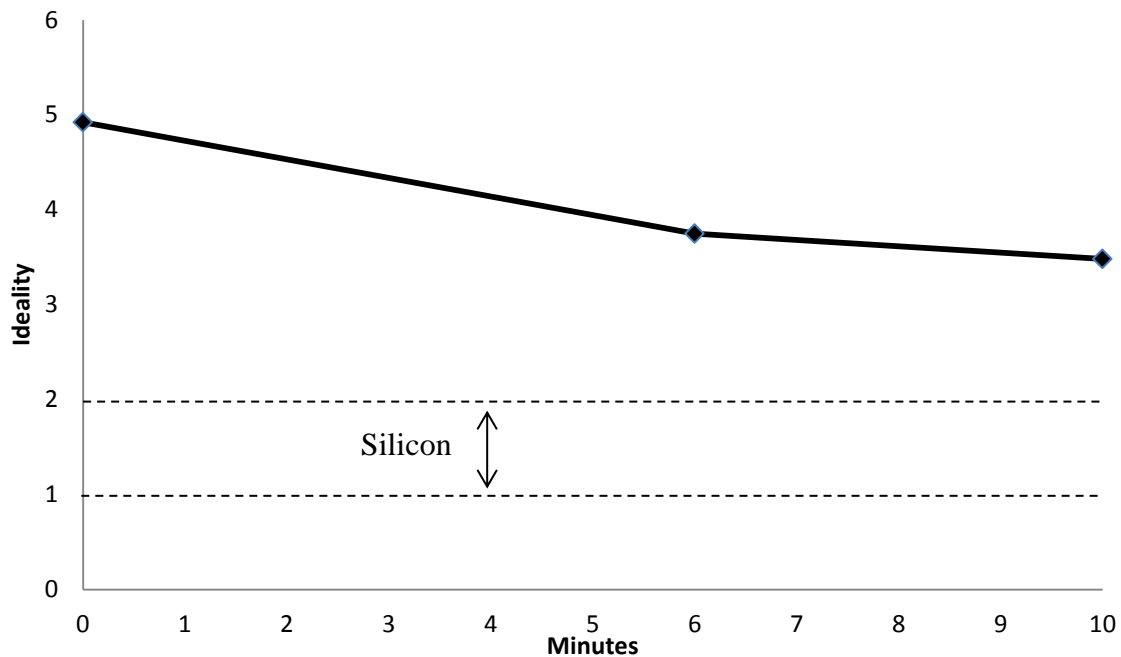


Figure 29. Ideality vs. Drying Time.

Ideality is a measure of the traps that prevent charge carriers from traversing the diode. Increased drying time results in stronger inter-chain interactions and growth of a more crystalline film, reducing the number of traps, which is confirmed by the ideality values decreasing from five (5) at zero (0) minutes, to 3.48 at 10 minutes drying time.

### 5.2.1.2. Annealing Temperature and Time in Ambient Air

Solution processed polymer diodes are annealed primarily to improve packing and reduce stresses from within the molecules, greater annealing temperatures and times may increase the crystallinity of the diodes.

J-V characteristic measurements were made to determine the effect of annealing time and temperature on the electrical characteristics of the diodes. The results were plotted to compare the trends of annealing time along with temperature.

## Example Characteristic Curve

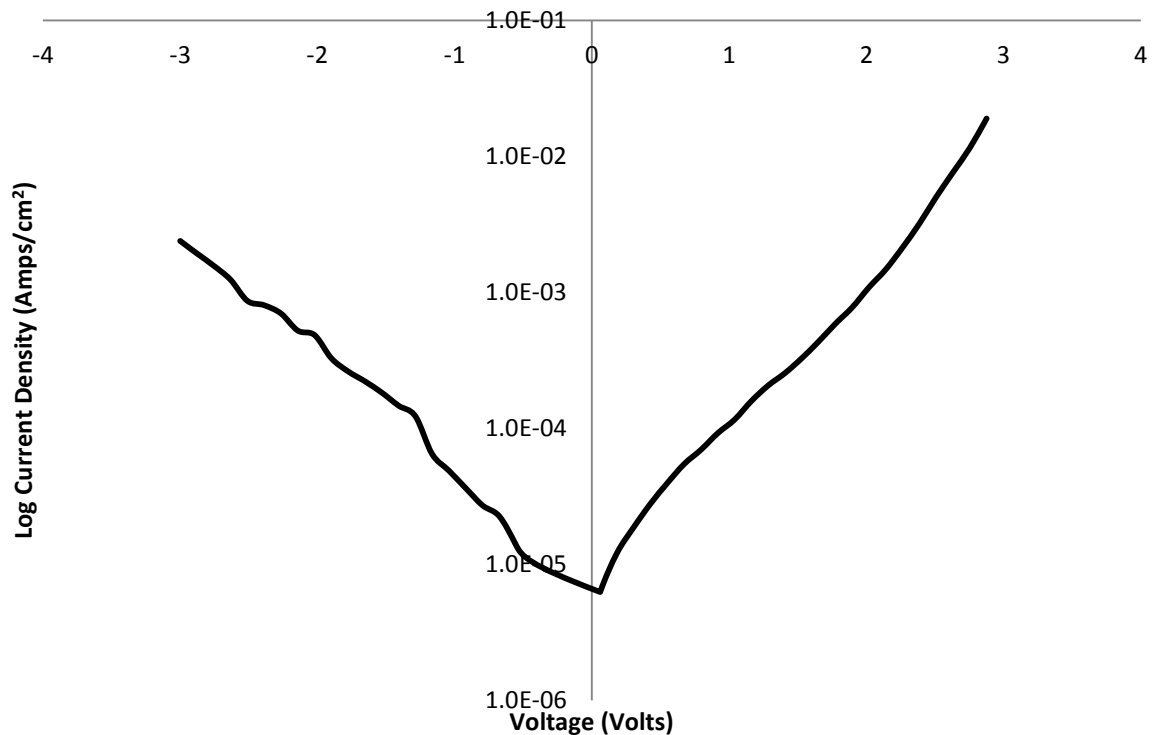


Figure 30. An example of a logarithmic Characteristic Curve from the data series (Annealed at 150°C for 20 minutes)

A set of devices were made under the conditions as in 4.1.2 Device Fabrication Recipe, with a standard drying time of five (5) minutes. The maximum temperature of 150°C was chosen as it is a standard annealing temperature for P3HT. The glass transition temperature for P3HT is -16 to 24°C [57], so minor chain rearrangement may occur at lower temperatures as well. The electrical properties; series and shunt resistance, rectification ratio and ideality were calculated and plotted to investigate their relationship with annealing temperature and time in inert conditions. The electrical property values of a diode from the previous section were added to the figures for comparison. The values come from the diode which was dried for six (6) minutes and annealed at 90°C for 20 minutes.

### Series Resistance

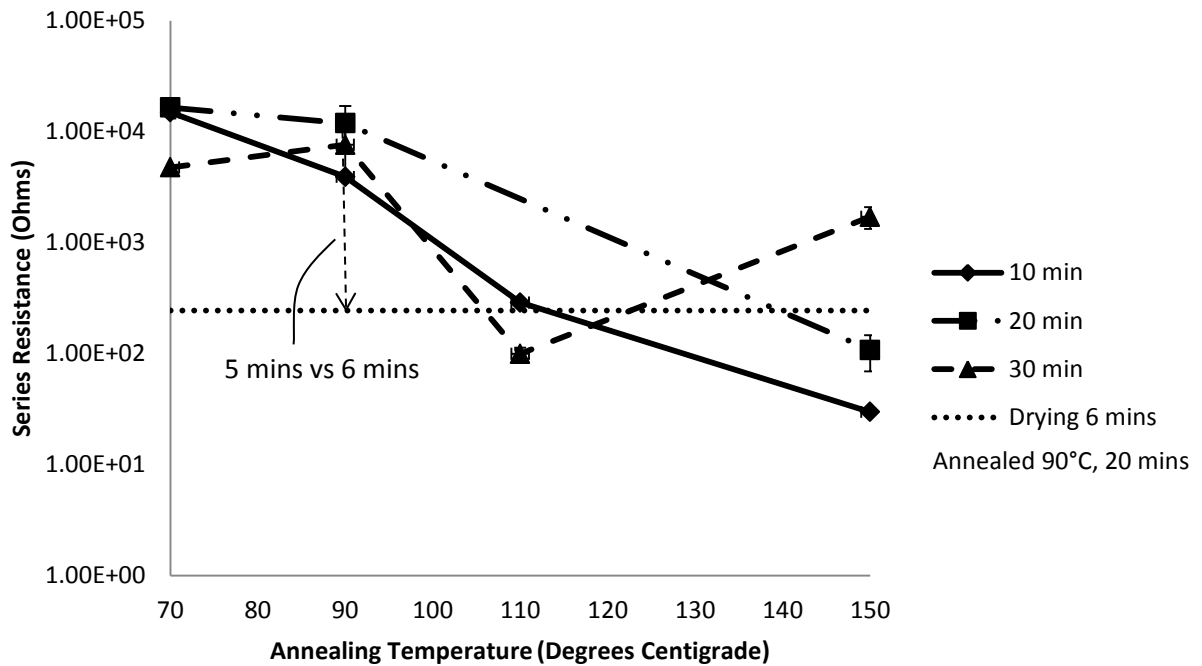


Figure 31. Series Resistance vs. Annealing Temperature (Annealing Time Series)

Series resistance from annealing, changes significantly over the 70°C to 150°C range. At 70°C the resistances are quite high in the ten of kilo-ohms range. A sharp decrease occurs between 90°C and 110°C as shown in Figure 31, and the series resistance continues to decrease with exception of 150°C annealed for 30 minutes.

An overall trend can be seen with the series resistance decreasing as the annealing temperature increased. Some exceptions to this trend were a significant outlier annealed at 150°C and for 30 minutes which is much higher than the other samples at the same temperature.

The sample dried for six (6) minutes is most comparable to the diode fabricated at 90°C for 20 minutes, however the value for the six (6) minute dried diode was much lower (244 Ω), than the diode dried for five (5) minutes in this set with a series resistance of 7620 Ω. Although following the same trend of decreasing series resistance with greater drying time, the one (1) minute longer drying time makes a significant difference in series resistance.

A longer annealing time will allow for polymer rearrangement leading to the expectation of a reduced series resistance. The series resistance seems unaffected by the annealing time with no particular trend, it appears that the drying time of five (5) minutes dominates

crystallisation and there is little to no gain from greater annealing times greater than 10 minutes.

## Shunt Resistance

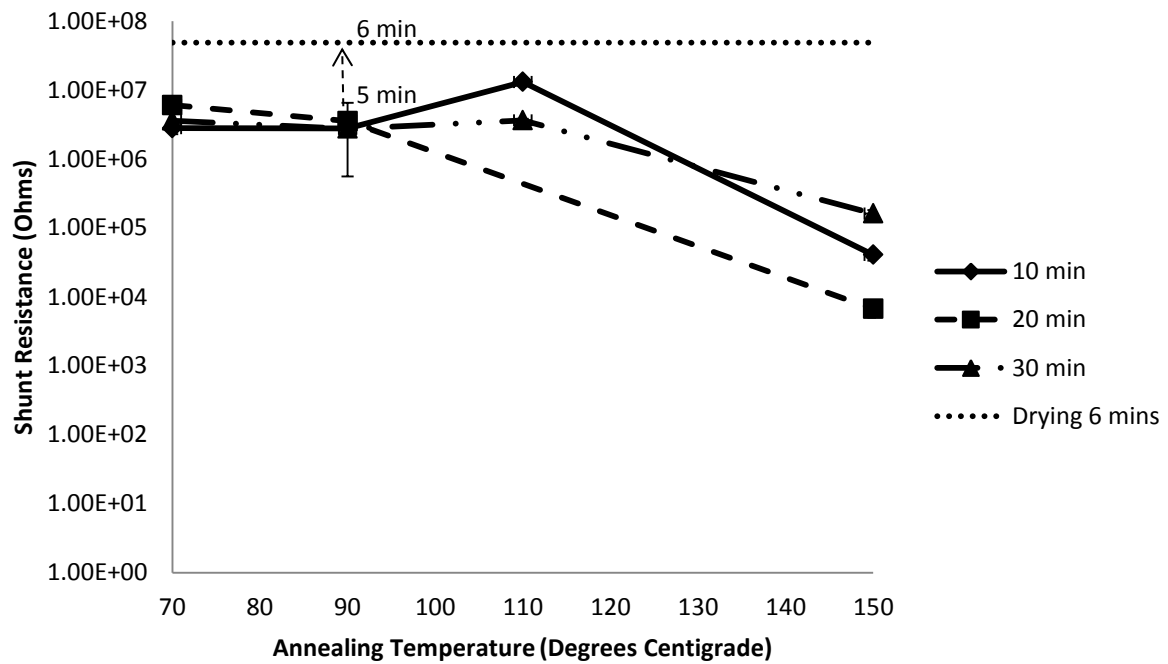


Figure 32. Shunt Resistance vs. Annealing Temperature (Annealing Time Series).

The shunt resistance decreased in the range of two orders of magnitude over the annealing range of 70°C to 150°C (Figure 32). As the annealing temperature is increased the shunt resistance decreases; a lower shunt resistance has a negative impact on the rectification and therefore decreases performance of the diodes.

The diode annealed at 90°C for 20 minutes had a shunt resistance of 3.54 MΩ has the most similar fabrication parameters, to the sample dried for six (6) minutes (horizontal line in Figure 32) with a shunt resistance of 48.8 MΩ. These results indicate that longer drying times increased the shunt resistance, however higher annealing temperatures decreased shunt resistance. Longer annealing time should allow for more rearrangement and crystallisation of the polymer, therefore decreasing the shunt resistance. However there is no significant variation in the shunt resistance data series, it appears the drying time dominates the rearrangement and crystallisation with little to no rearrangement or crystallisation occurring due to greater annealing times.

## Rectification Ratio

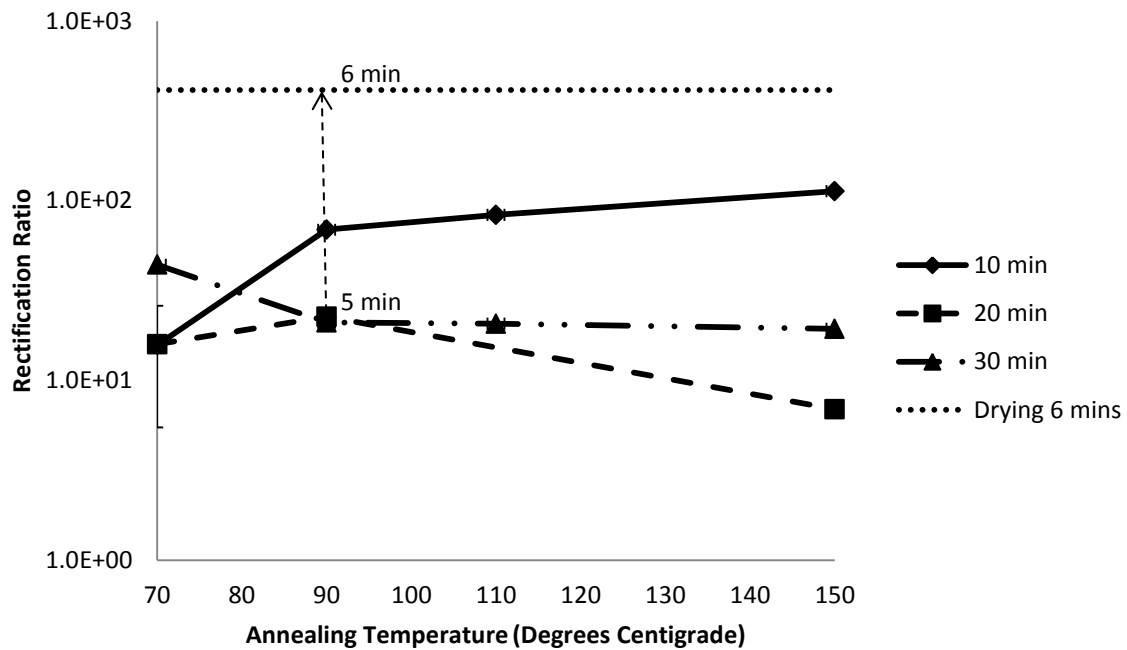


Figure 33. Rectification Ratio vs. Annealing Temperature (Time Series).

Annealing appears not to significantly impact the rectification ratio of diodes annealed in air. Diodes annealed for 20 and 30 minutes have an overall decreasing trend with increasing annealing temperature, while an increase in rectification ratio was observed for the diodes annealed for 10 minutes over the same range. A proportional decrease both in the shunt and series resistances as annealing temperature increases has resulted in a relatively stable rectification ratio.

The rectification ratio (414 : 1) of the sample dried for six (6) minutes and annealed at 90°C for 20 minutes is much greater than the devices fabricated in this annealing series. The diode fabricated with the same conditions except for (5) minutes drying time resulted in a rectification ratio of 22.6 : 1 which is even lower than the interpolated point of five (5) minutes of ~100 : 1 from Figure 28.

## Ideality

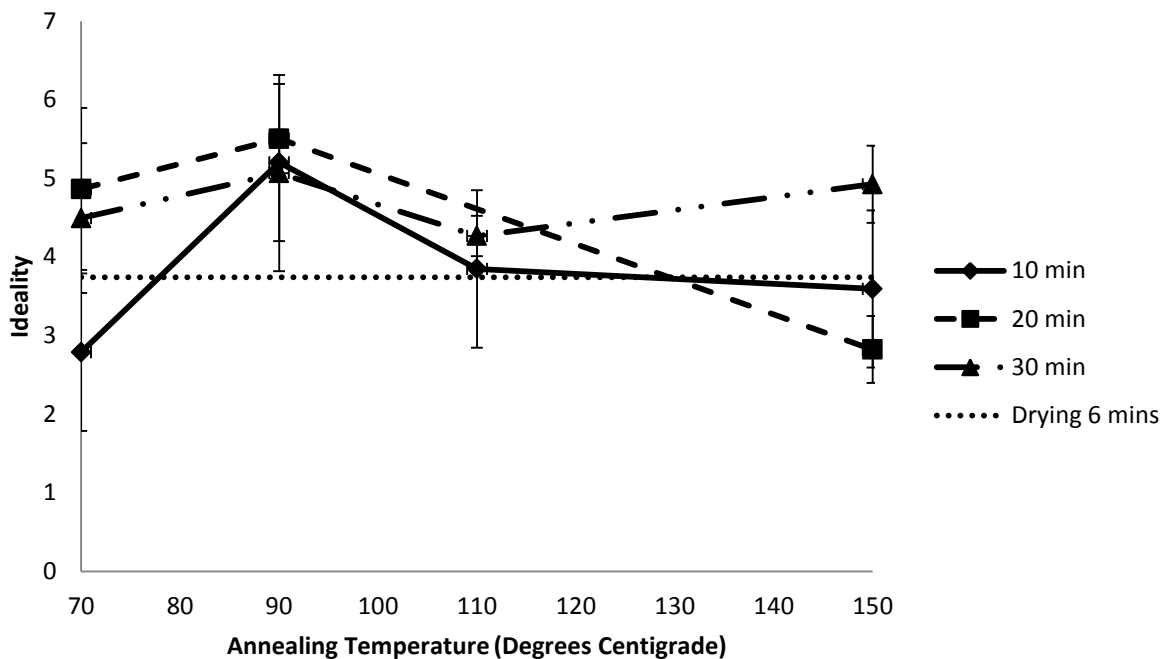


Figure 34. Ideality vs. Annealing Temperature (Annealing Time Series).

In Figure 34 the ideality values of diodes were calculated for annealing temperatures ranging from 70°C to 150°C and fell in a range from 2.7 to 5.5 which fall within the standard range of ideality values for organic diodes. However, there was no clear correlation between annealing temperature and ideality (within error) over the temperature range. Except for diodes annealed at 150°C, the ideality increased as annealing time increased, inferring more recombination occurs in diodes annealed for longer periods.

Annealing should improve the packing and relieve stress from within the molecules resulting in a slight increase in crystallinity. Minor changes in the electrical properties can be seen such as the decrease in series resistance and shunt resistance. However, it appears that most of the improvement in electrical properties has occurred during the drying stage and that little further improvement is observed from longer annealing times or higher annealing temperatures.

## 5.2.2. Fabrication of Devices in an Inert Environment

### 5.2.2.1. Drying Time

Drying time plays a significant role in determining the electrical properties of diodes therefore a comparison was undertaken with devices prepared under inert conditions. The chosen conditions were 90°C annealing time for 20 minutes with 5 minutes drying time, because they provided the greatest electrical properties for devices annealed in air. The devices were tested in air under the same conditions, five cycles were taken and the average of the last four was used for the data analysis.

#### Comparison of devices in annealed in Air and Inert conditions.

Annealing / Error	Air	Inert	$\Delta(\text{Inert} - \text{Air})$
Rectification (arb)	413 $\pm$ 252	629 $\pm$ 406	215
Series Resistance ( $\Omega$ )	204 $\pm$ 28	101 $\pm$ 4.35	-102
Shunt Resistance ( $\Omega$ )	363,000 $\pm$ 119,000	85,100 $\pm$ 12,000	-278,000
Ideality (arb)	10.7 $\pm$ 0.3	11.3 $\pm$ 0.9	0.5

Table 2. Comparison of annealing devices in Air and Inert environments with 5 minutes Drying Time.

Table 2 demonstrates the differences between diode fabrication in air and inert conditions for five (5) minutes of drying time. Minor improvements in the rectification and series resistance were observed while other electrical parameters worsened by minor amounts.

An inert environment was expected to display some rectification because P3HT is an intrinsic semiconductor. An excellent diode was expected to be fabricated with no air or moisture doping or changing energy levels or the P3HT.

There is only a slight overall improvement in the diodes produced in the inert environment. A greater number of diodes per device perform as diodes being attributed to the cleaner environment.

### 5.2.2.2. Annealing Temperature in Inert Environment

A set of devices were made according to Device Fabrication. The drying time ( $t_{\text{drying}}$ ) was kept at 5mins and devices were annealed at a range of temperatures  $T_{\text{Anneal}}$  90°C, 100°C, 113°C, 122°C and 130°C for 20 minutes. The annealing temperature range was chosen similar to the devices fabricated in Air. The devices from the annealing temperature range were tested in Air.

#### Series Resistance

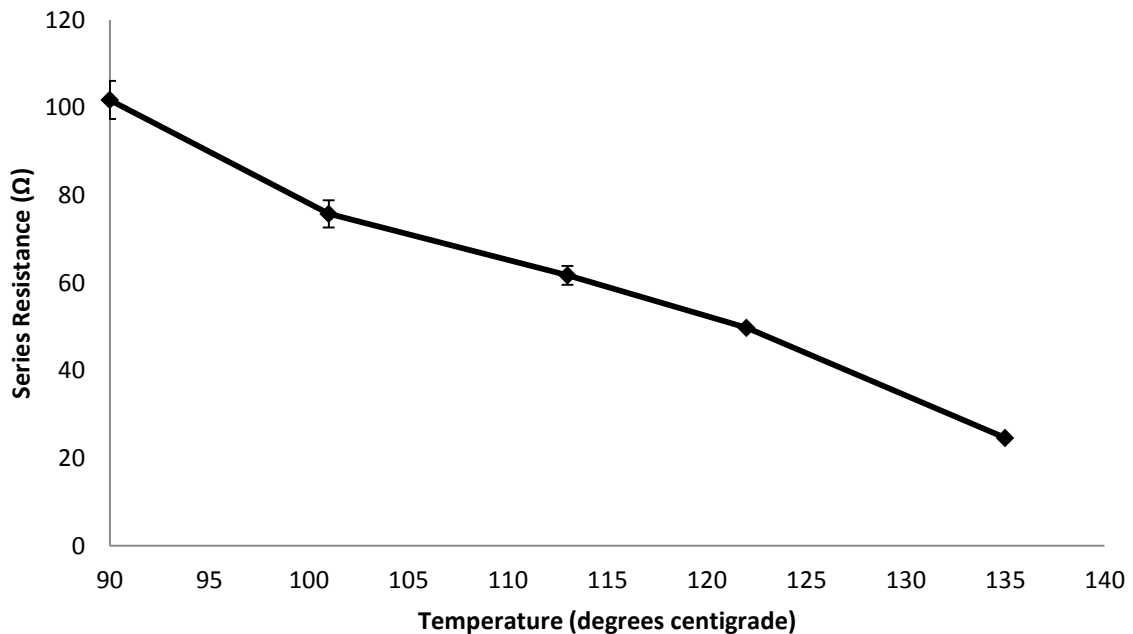


Figure 35. Series Resistance vs. Annealing Temperature in an Inert Environment.

The y-axis of Figure 35 displaying series resistance is not exponential so the variation and values are much less compared to the series annealed in air. Series resistance linearly decreases as the annealing temperature was increases from 102 Ω at 90°C to 24.6 Ω at 135°C.

Inert fabrication improved the electrical properties of the diodes compared to ambient fabrication; the series resistance of the diodes improved due to less interaction with oxygen and water. The series resistance of the diodes decreased with the annealing temperature similar to the devices fabricated in air. However, the series resistances in Figure 35 are far

smaller than the devices annealed in air, alluding to the conclusion that annealing in an inert environment vastly improves the series resistance of devices.

### Shunt Resistance

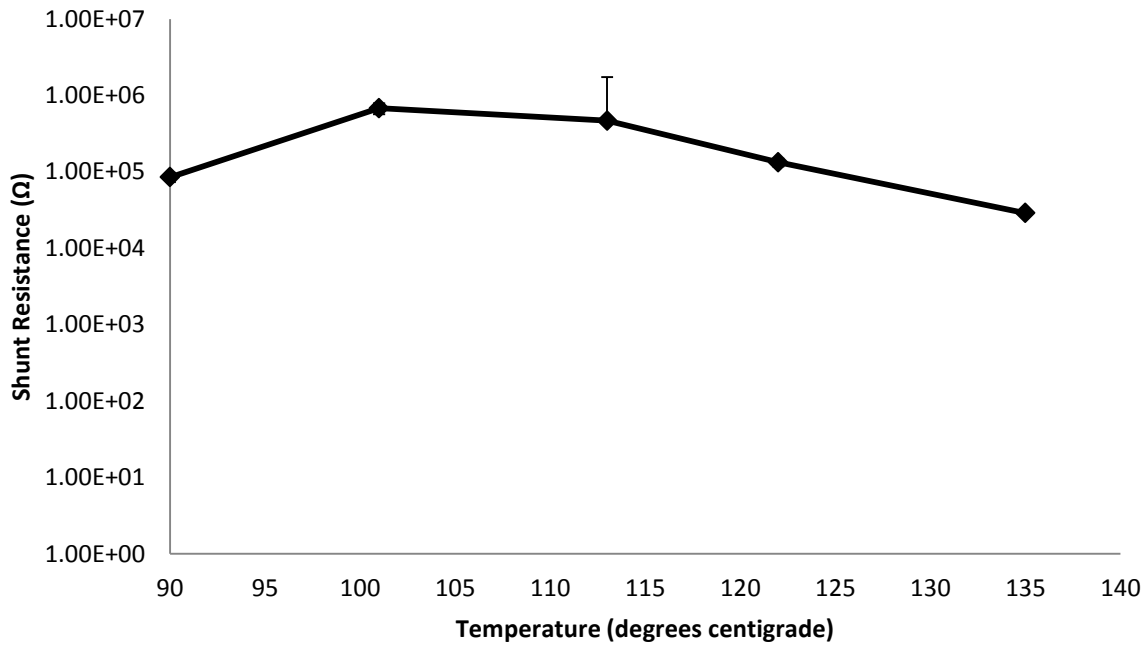


Figure 36. Shunt Resistance versus Annealing Temperature in an Inert Environment.

Inert fabrication was expected to improve the device due to the lack to interaction with oxygen and water. Unlike air fabricated diodes, the shunt resistance increased as annealing temperature increased and then decreased above 100°C. The shunt resistances of diodes in Figure 36 remained in the lower end of the range of the diodes annealed in air, with the maximum at 680 KΩ at 100°C and minimum at 28 KΩ. The lower shunt resistance of devices fabricated in inert conditions is detrimental to the overall performance of the diodes.

## Rectification Ratio

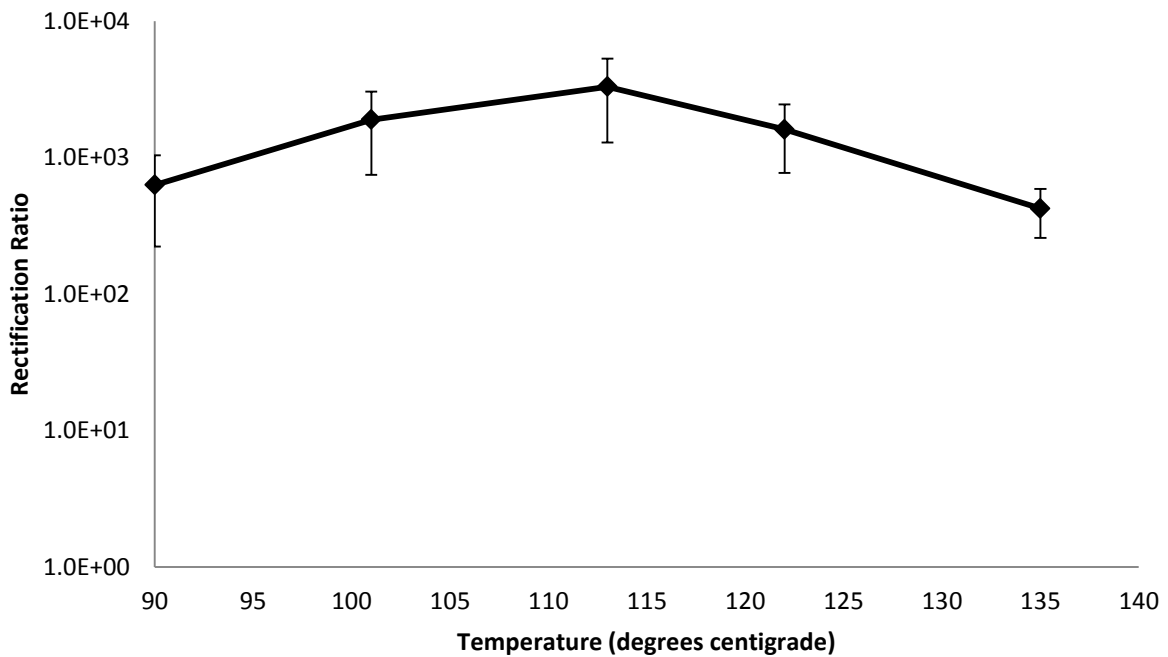


Figure 37. Rectification Ratio versus Annealing Temperature in an Inert Environment.

Rectification ratio was expected to increase with annealing temperature (as with ambient fabricated devices) due to the decrease in series resistance (Figure 37). However shunt resistance dominates the rectification ratio for the diodes fabricated in inert conditions and therefore results in a similar trend. The series resistance does not vary much when compared to the shunt resistance explaining the similarity and dependence on the shunt resistance. The rectification ratios have improved greatly from the diodes annealed in air but are now dominated by the lower shunt resistance rather than the series resistance.

## Ideality

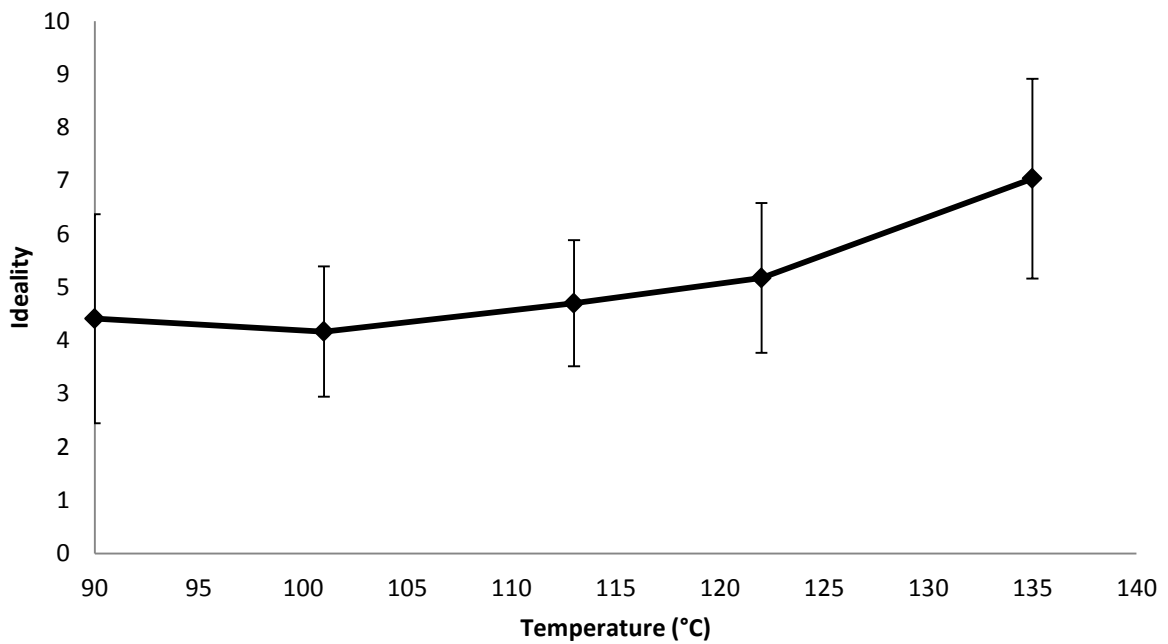


Figure 38. Ideality vs. Annealing Temperature in an Inert Environment.

A greater annealing temperature will reduce intra-polymer stresses especially as the glass transition temperature is reached. The ideality slightly increases between 90°C to 135°C as shown in Figure 38 however the values are similar within the calculated error ranges. At the minimum temperature the diodes are more accurately described by the Schottky diode equation.

### **5.2.3. Controlled Environment Device Testing**

It is well known that both P3HT and Aluminium are sensitive to air, particularly oxygen, P3HT is an intrinsic p-type semiconductor, meaning it has a full HOMO and empty LUMO. Latent thermal energy will excite some electrons into the LUMO and generate holes in the HOMO resulting in semiconducting properties but the small number of majority charge carriers (holes) will result in a very low conductivity. However, oxygen forms a charge transfer carrier with P3HT which increases the number of charge carriers and therefore conductivity of P3HT.

Aluminium metal readily oxidizes in atmospheric conditions altering the work function. Aluminium oxide has a higher work function of  $\sim 6.7$  eV [58] compared with Al at  $\sim 4.1$  eV [58] altering the metal-semiconductor interface and impacting the electrical properties. If oxidation should occur at the junction of aluminium and P3HT then diode electrical properties would be affected, which could be beneficial or detrimental depending on the design of the diode. Oxidation at any other surface could introduce a contact resistance which may manifest itself as either diode due to the formation of a dipole at the interface or an increase in the series resistance.

Two methods of controlling the environment around the devices were tested; Firstly encapsulation that completely seals the device as produced. Secondly a small glove box was built to maintain an inert environment as the devices were tested.

#### **5.2.3.1. Encapsulation**

The Schottky diodes were fabricated in the manner according to Device Fabrication with exception that the device was placed on the hot plate directly after spin coating. The sample was tested in air by ramping from -4 volts to +4 volts and a difference can be seen where the current decreases over multiple tests. The sample was returned to the glove-box and sealed with a glass slide and UV-curable glue to prevent any further ingress or egress of air and moisture.

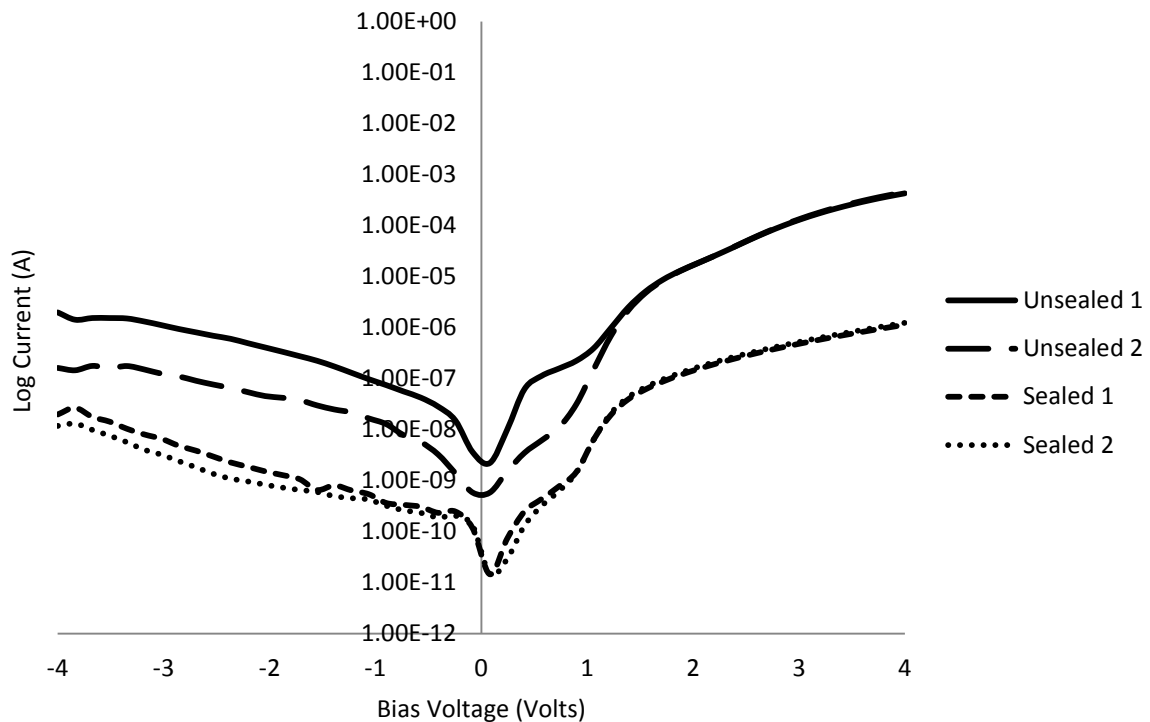


Figure 39. Diode behaviour before and after encapsulating.

J-V characteristic curves of a diode before and after encapsulation are shown in Figure 39. Curves “Unsealed” 1 and 2 are from pre-encapsulation and curves are post encapsulation. Variation in the current can be seen between ‘Unsealed’ one and ‘Unsealed’ two, primarily the reverse current decreased resulting in the shunt resistance increasing, improving the rectification ratio. However, the overall current reduced between initial testing and after encapsulation. Steps in the process of encapsulation have possibly affected the electrical properties of the diodes. The encapsulation glue is cured with UV-light which could affect the P3HT doping. However encapsulation is undertaken in the glove box causing the removal of oxygen from the P3HT layer. Removal of oxygen from the atmosphere around the diodes could cause oxygen to migrate out of the diodes. A lower amount of oxygen in the P3HT would result in less charge transfer complexes to provide holes for conduction.

Encapsulation appears to be very effective at stabilising the diodes electrical properties. The diodes were no longer in contact with the external environment, specifically the oxygen and water in the air. The slight difference in the characteristic between the two tests after encapsulation is likely due to migration of O<sub>2</sub> in the polymer suggesting air continues to affect the diodes after fabrication and not just during fabrication.

Encapsulated samples were tested to isolate the effect of air but the process introduced two new variables the UV-curable glue and the exposure of the sample to UV Light. To exclude

the encapsulation process as a factor an inert testing environment was devised to control the environment while testing.

### 5.2.3.2. Inert Testing Environment

A smaller glove-box was designed and made to transfer and test samples from the fabrication glove-box to the electrical testing room. The testing glove-box was designed to enter the large antechamber of the large glove box so that samples can be transferred into the testing glove-box. This was to achieve an entirely dry and inert environment from fabrication to testing without breaking this environment. A testing rig built into the bottom of the box allows mounting of the sample while testing. Eight connecting wires are fed through to banana plugs to form the electrical connections.

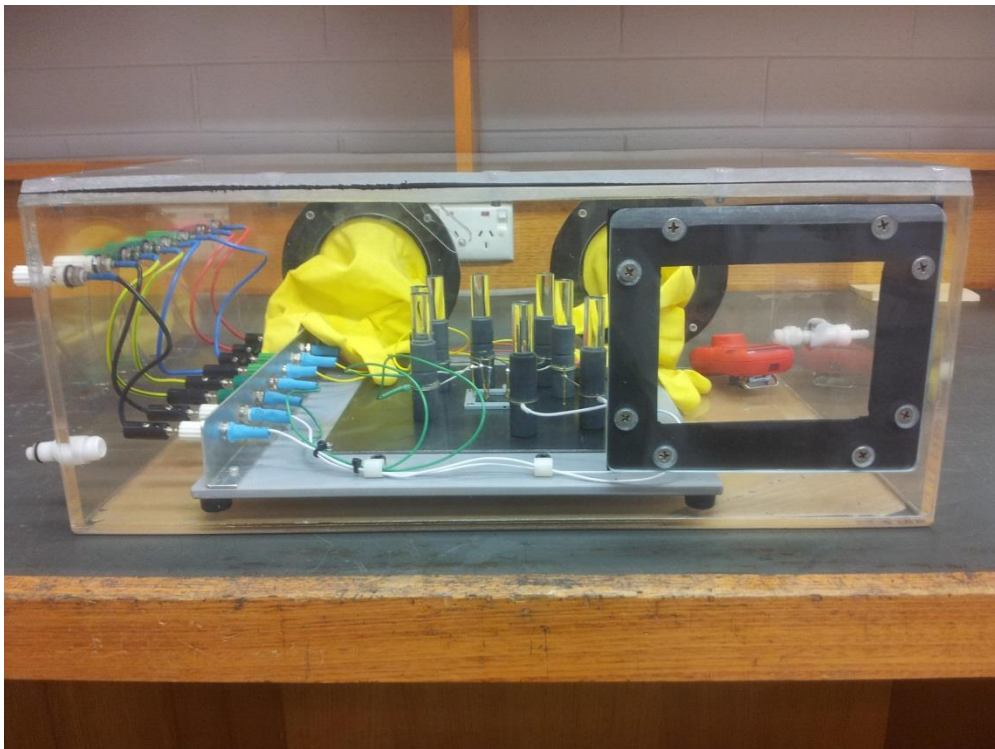


Figure 40. Electrical Testing Glove-box.

### 5.2.3.3. Effect of Air on Device Electrical Properties

The Schottky diodes were fabricated in the manner according to 4.1.2 Device Fabrication with the exception that the aluminium was deposited on the glass as the bottom electrode and gold electrode was deposited on top of the polymer layer. The diodes were transferred to the testing glove box J-V characteristic curves were collected in the glove box by ramping from -4 volts to +4 volts.

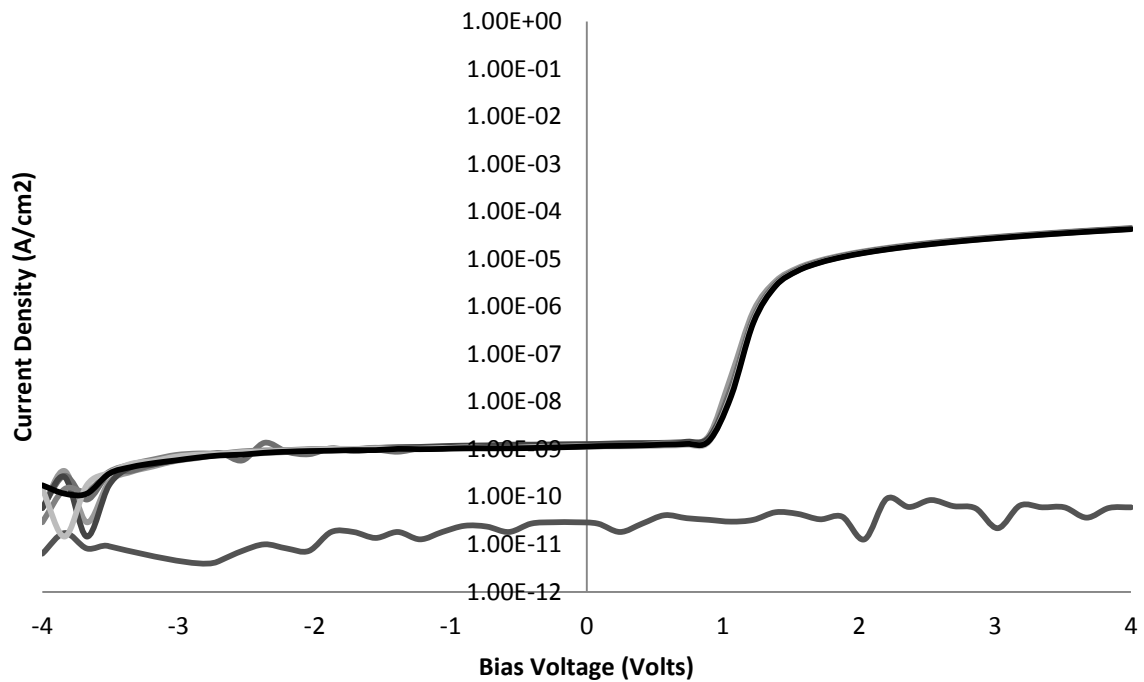


Figure 41. J-V Characteristic curves of a diode before and after exposure to 0.1% air. Initial testing resulted in open circuit J-V characteristic as seen in Figure 41. Air was then admitted into the box for 1 minute and then purged with nitrogen resulting in 0.1% oxygen per volume; the device began to perform as a diode with currents in the orders of  $1 \times 10^{-9}$  -  $1 \times 10^{-4}$  Amps.

A critical observation made from inert fabrication and testing is that the diodes did not display any rectification unless exposed to air. P3HT is an intrinsic semiconductor and a junction between Al and P3HT should form a metal-semiconductor barrier which would behave as a Schottky diode. However, the mobility of undoped P3HT is very low ( $10^{-5}$  -  $10^{-4}$   $\text{cm}^2/(\text{V}\cdot\text{s})$ )[59], resulting in a current to below the detection limit of the Keithley 2400.

Rectification Ratio	$7.49 \times 10^5 : 1$	
Series Resistance	$6.21 \times 10^4$	Ohms ( $\Omega$ )
Shunt Resistance	$1.94 \times 10^9$	Ohms ( $\Omega$ )
Ideality	2.11	

Table 3. Electrical Properties of controlled doped P3HT/Al diode.

After exposure to 0.1% air for 1 minute the device showed very strong diode performance despite low conductivity. Table 3 is a summary of the diodes electrical properties. The resistances are very high compared to other devices, but this is to be expected due to the low level of doping. The high series resistance at 60 K $\Omega$  will disadvantage the rectification ratio but the significantly higher shunt resistance at almost 2 G $\Omega$  more than compensates resulting in a rectification ratio of  $7.5 \times 10^5 : 1$ . An ideality of 2.1 is the lowest of all the devices meaning it is well described by the Shockley diode model and also infers there is little recombination.

The impressive electrical properties of the diode demonstrate the importance of controlled doping in these diodes. Unfortunately controlled doping with oxygen is very difficult to achieve, despite excellent stability over an hour of constant testing, oxygen is likely to diffuse in and out of an encapsulated device, limiting practical application.

#### 5.2.3.4. Effect of Bias Voltage on Device Performance

Large bias voltages in the order of tens to hundreds of volts have reported to have an effect on depleting P3HT bulk polymer to reduce the off current in transistors[60]. The large voltages have the potential to alter the chemical and structural/morphological nature of the devices and affect the electrical properties.

A device was made and was kept in an inert nitrogen environment. The device was then transferred to a miniature glove-box and electrically tested. An initial I-V curve of +/- 4V was recorded. A voltage was applied for 5 seconds, then another I-V curve was taken to record any changes the application of voltage may have induced.

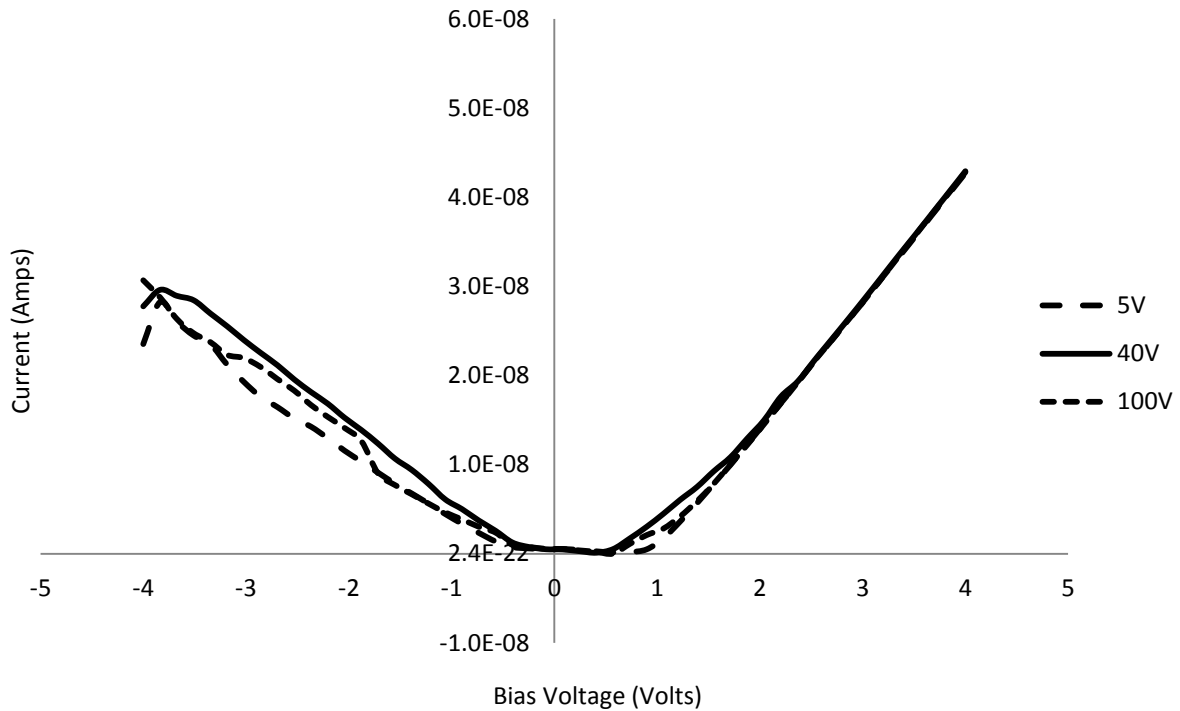


Figure 42. The bias voltage was increased sequentially from +5V until +100V was reached with an I-V curve taken each time only 5V, 40V and 100V are shown for clarity.

The device did not become doped due to the high voltages and remained a very poor diode. The same result was found with sequentially negatively biasing and recording I-V curves on a separate diode.

The I-V curves of the devices were all insulating with current in the order of  $1 \times 10^{-9}$  Amps. No changes were observed for devices under an inert nitrogen environment. Despite the very large voltages these characteristic curves did not change significantly. It is reasonable to conclude that bias voltage does not alter devices prepared and tested under inert conditions. The results of Singh et.al[61] attempted these same experiments in air and had success but could not be reproduced in an inert atmosphere.

## 5.3. Device Parameters

### 5.3.1. Diode Area

A set of devices were made according to 4.1.2 : Device Fabrication Recipe, with five (5) minutes drying time and 20 minutes annealing time at 90°C. The evaporation mask was designed for three different sized diode areas, 0.01cm<sup>2</sup>, 0.015 cm<sup>2</sup> and 0.027 cm<sup>2</sup>. However, the aluminium evaporated on to the glass as the bottom electrode and gold was evaporated on top of the annealed polymer as the top electrode. The electrical parameters series resistance, shunt resistance, rectification and ideality were calculated without area normalisation to investigate their direct relationship to diode area.

#### Series Resistance

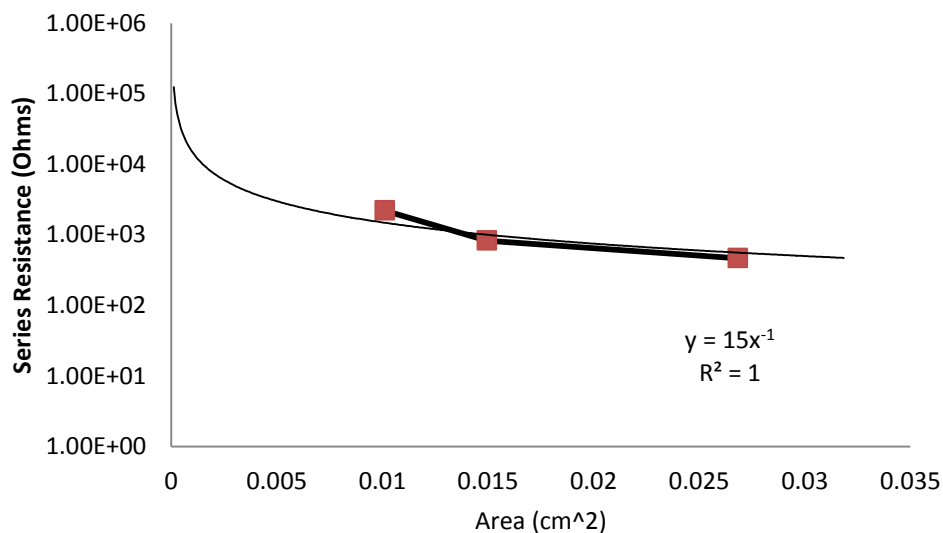


Figure 43. Series Resistance vs. Diode Area.

Series resistance is inversely proportional to diode area, a trend-line of  $y = k/x$  was plotted (Figure 43). The Richardson equation ( $J_0 = AA*T^2 \exp(\frac{-q \phi_b}{kT})$ ) states current is directly proportional to diode area, and series resistance is inversely proportional to current ( $r = \frac{V}{I}$ ), therefore series resistance is inversely proportional to electrode area  $r \propto \frac{k}{A}$ .

## Shunt Resistance

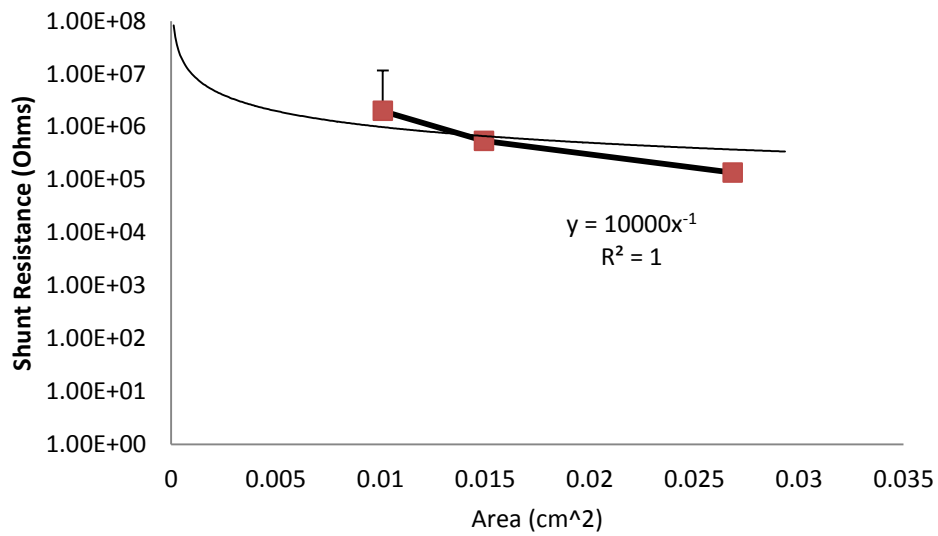


Figure 44. Shunt Resistance vs. Diode Area.

Similarly, shunt resistance is inversely proportional to diode area, a trend-line of  $y = k/x$  was plotted with a constant of proportionality of 10000 (Figure 44). The data follows the trend-line although not as tightly as the series resistance.

## Rectification Ratio

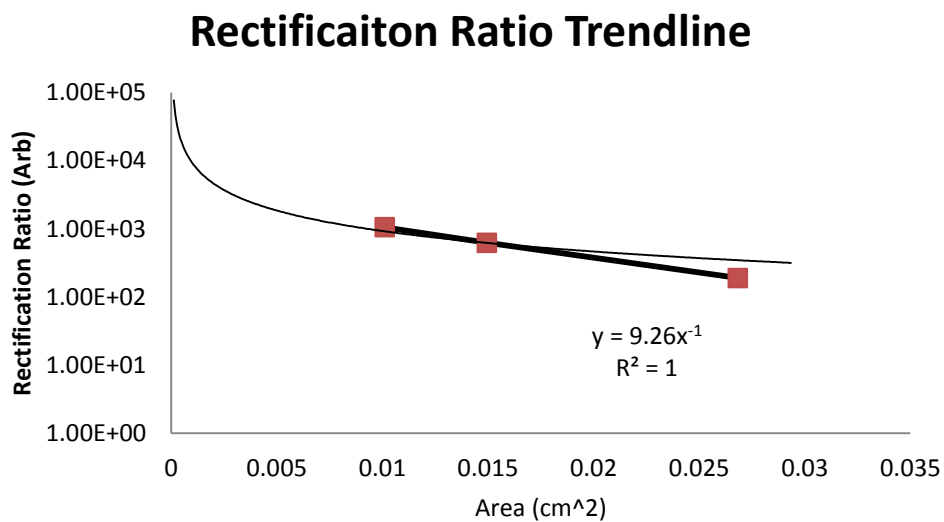


Figure 45. Rectification vs. Diode Area.

Figure 45 shows the rectification ratio decreased from 1,047 : 1 for the smallest diode (0.01 cm<sup>2</sup>), to 619 : 1 for the diode with 0.015 cm<sup>2</sup> area, and 189 : 1 for the largest diode with 0.027 cm<sup>2</sup> diode area.

The calculation of rectification does not include area because it is a ratio between the forward and reverse current at a chosen bias voltage, for these experiments the voltage was ± 4 Volts. However the rectification ratio appears to be negatively proportional to the electrode area of the diodes, this appears to be due to the trends that the shunt and series resistance follow.

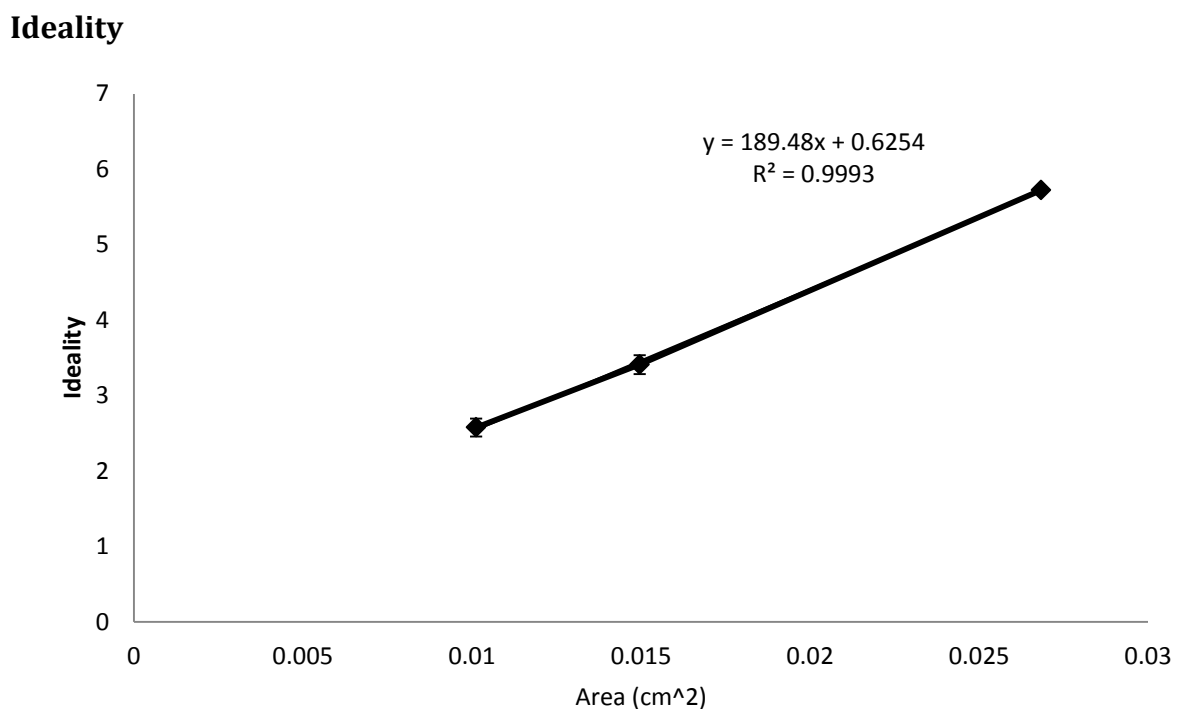


Figure 46. Ideality vs. Diode Area.

Figure 46 shows ideality linearly increases as the area of the diode increases, inferring smaller diodes are increasingly well modelled by Schottky equation. A linear fit gives the slope as 189.48 and the intercept as 0.63 with an R-squared value as 0.9993. The linear fit results in a y-intercept of 0.63 which is below ideality, resulting in an “impossible” fit to the Shockley diode model. The linear fit corresponds to an ideality of 1 ( $y = 1$ ) at 0.0020 cm<sup>2</sup>, considering this value, diodes with a layered structure and rectangular contacts, an ideal diode would have an electrode area of 0.0020 cm<sup>2</sup>.

### 5.3.2. P3HT Layer Thickness

The diodes were fabricated with the process from chapter 4.1.2 : Device Fabrication Recipe, the polymer layers were left to dry for five (5) minutes and annealed at 90°C for 20 minutes. Polymer layer thicknesses and errors of the layers were measured and calculated. The electrical properties were extracted for devices with a range of P3HT layer thickness.

#### 5.3.2.1. Thickness Measurement of P3HT Layers

A set of devices were fabricated without electrodes, three score marks were made with a scalpel blade in the polymer layer, the difference in height of the scratch mark and the top of the nearby P3HT layer was measured by AFM (Atomic Force Microscopy) to calculate the thickness of the P3HT layer (Figure 47). The devices were prepared in the same fashion as the diode fabrication except no electrodes were deposited. Nine devices fabricated from combination of three solution concentrations and three spin speeds. The devices were then cut down to  $\sim 1\text{cm}^2$  squares to fit into the AFM. Three lines were scratched with a scalpel blade in each device to measure the step height from the substrate to the top of the polymer layer. The process used for analysing the images involved a 0<sup>th</sup> order flatten image due to the flat nature of the devices. The step function was used to measure the height in two steps:

1. The measuring bars were all moved to the polymer side of the image and the level function was performed to level the image.
2. One pair of measuring bars was moved to the polymer side and the other to the substrate side and the height was recorded.

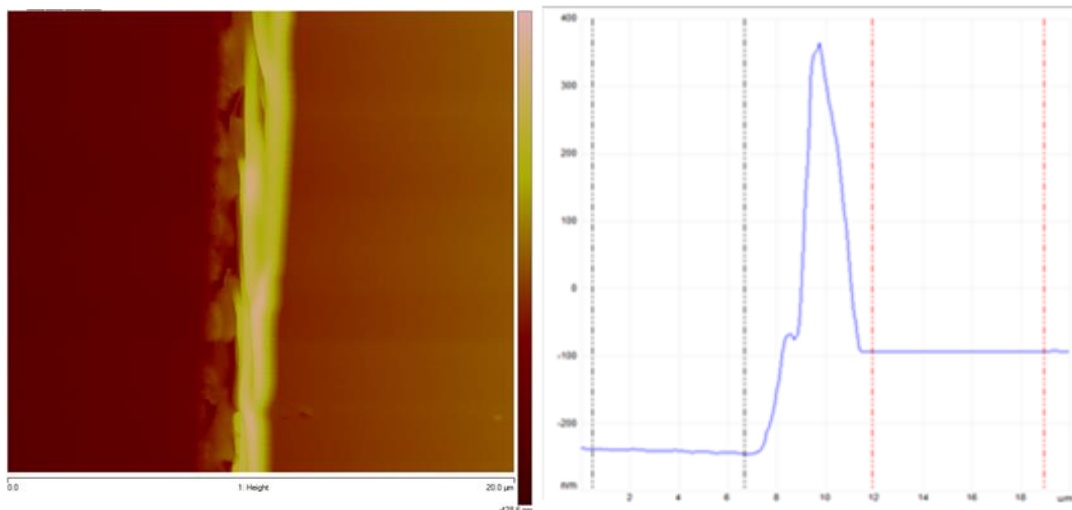


Figure 47. AFM image of a scratched step, the left side of the image is the glass which is lower than the polymer layer (Left image) and the step profile of the glass slide (left) with polymer layer (right) on top (Right image).

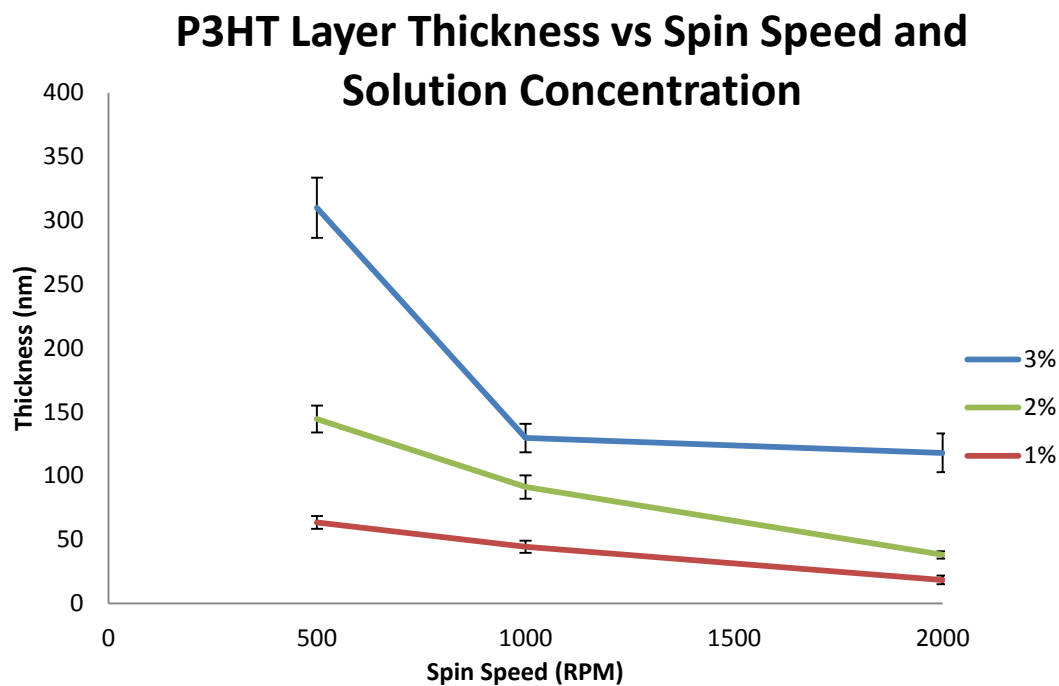


Figure 48. Graph of AFM thicknesses measurements of P3HT layer on Glass. The lines on the graph are only to guide the eye.

Sample #	Sol. Conc.	Spin Speed	A	B	C	Avg.	STD Dev.
1	3	2000	132	102	120	118	15.0
2	3	1000	138	117	134	129	11.1
3	3	500	327	320	283	310	23.6
7	2	2000	42	37	35.3	38.1	3.48
8	2	1000	94.6	87.9		91.2	4.73
9	2	500	141	148		144	4.94
4	1	2000	15.2	20.1	20.2	18.5	2.85
5	1	1000	41.2	54.8	37.6	44.5	9.07
6	1	500	56.1	70.9		63.5	10.4

Table 4. Thickness measurements of P3HT with various spin speeds and solution concentrations.

Figure 48 shows the results from the AFM thickness measurement. A correlation can be seen between spin speed and solution concentrations effect on polymer thickness. The thickness for 3% solution concentration at 1000 and 2000 rpm are closer than expected but taking the error into consideration the correlation is still quite strong.

A low amount of error is an encouraging result for this measurement as the thickness is a critical parameter of this project. Figure 47 shows the profile for a typical measurement taken a large spike can be seen in between the polymer and glass plateaus, this is organic material that is pushed up during the scratching procedure. The spike is difficult to avoid due to the method areas along the scratch have be found to minimise the spike. The spike should not affect the measurement dramatically because the plateaus heights are measured. The error decreases for thinner layers but it is not clear whether this is due to the peak or the variation in the thickness of the layer.

### 5.3.2.2. P3HT Thickness effect on Electrical Properties

#### Series Resistance

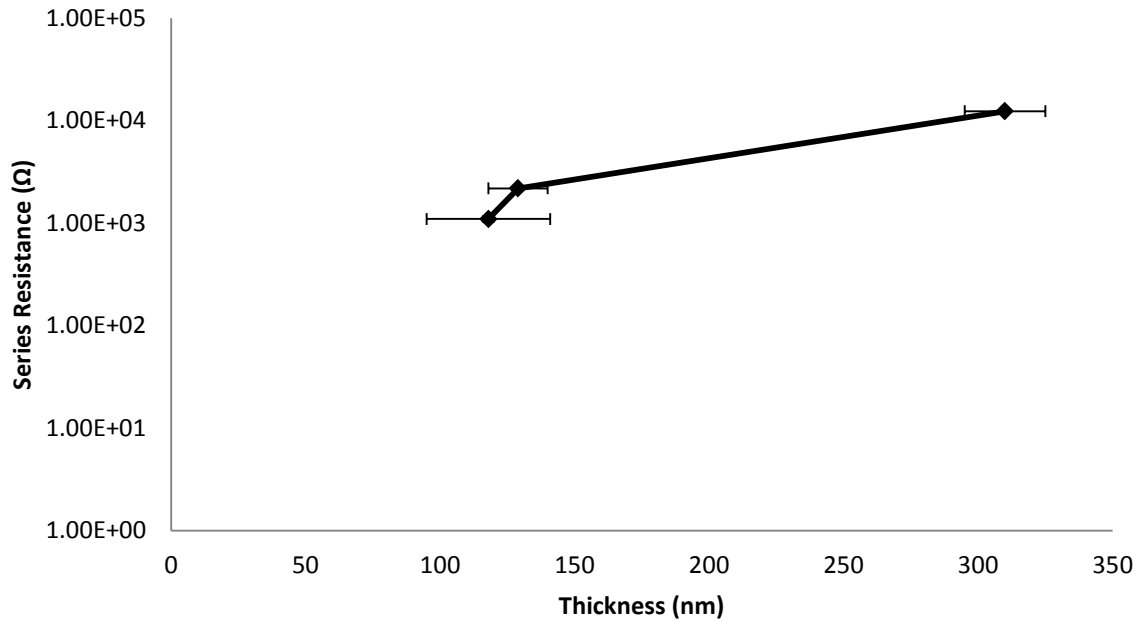


Figure 49. Series Resistance vs. P3HT Thickness.

Figure 49 shows the series resistance of the layers over the thickness range increased as the thickness of the layers increased. The primary factor that determines series resistance is conduction in the bulk of the polymer. Charge carriers have a longer path to travel in thicker bulk polymer layers. Series resistance is therefore expected to increase as the thickness of the polymer layer increased.

## Shunt Resistance

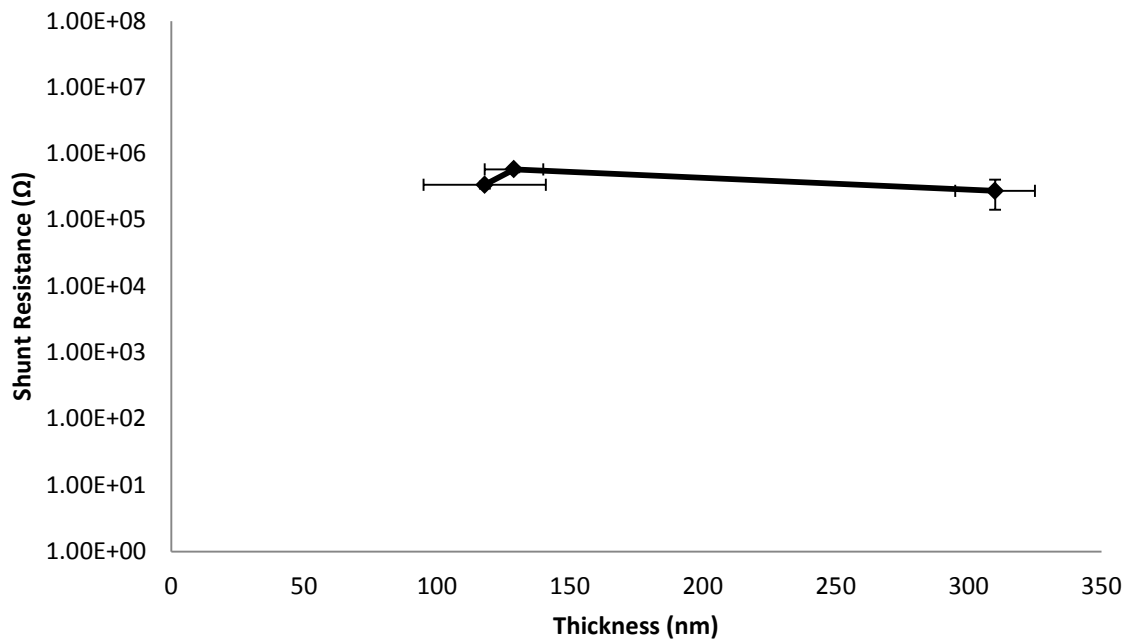


Figure 50. Shunt Resistance vs. P3HT Thickness.

The shunt resistances were all in the realm of  $10^5 \Omega$ , and appear almost unaffected by the thickness of the P3HT layer (within error) as shown in Figure 50. As the shunt resistance is a combination of the junction resistance and the resistance from the of the polymer layer, the shunt resistance would be expected to slightly increase as the thickness increased; but not as significantly as the series resistance.

## Rectification Ratio

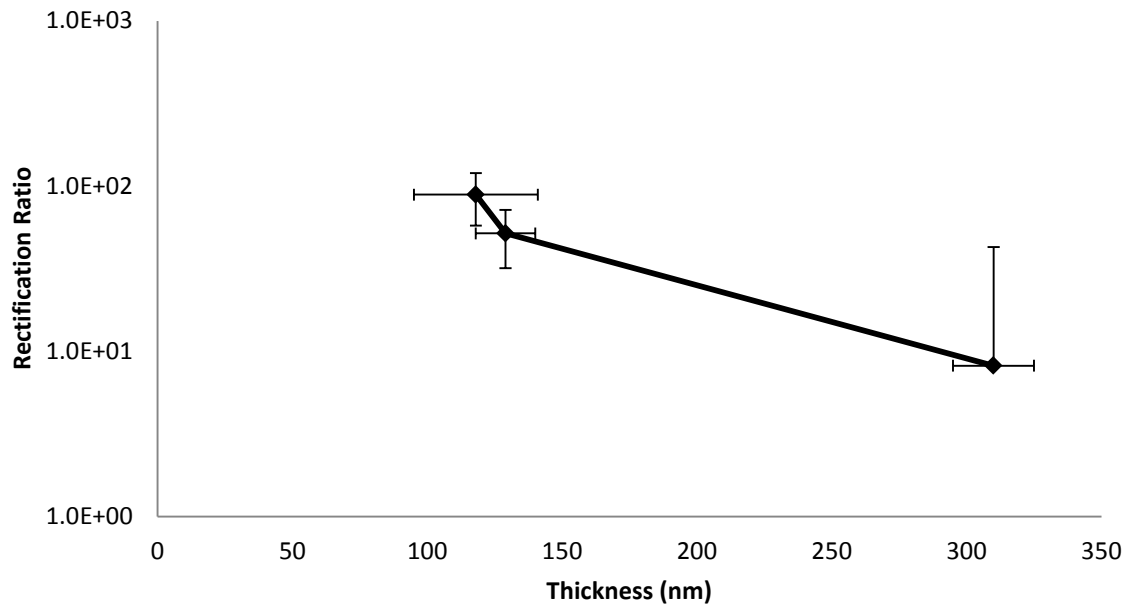


Figure 51. Rectification Ratio vs. P3HT Thickness.

The rectification ratio of the diodes decreases with greater polymer layer thickness within the 100 – 310 nm range (Figure 51). Shunt resistance was almost constant for all three samples but the series resistance greatly increased, reducing rectification ratios. A different relationship may occur for polymer layers in different ranges for example sub 50 nm and above 500 nm.

## Ideality

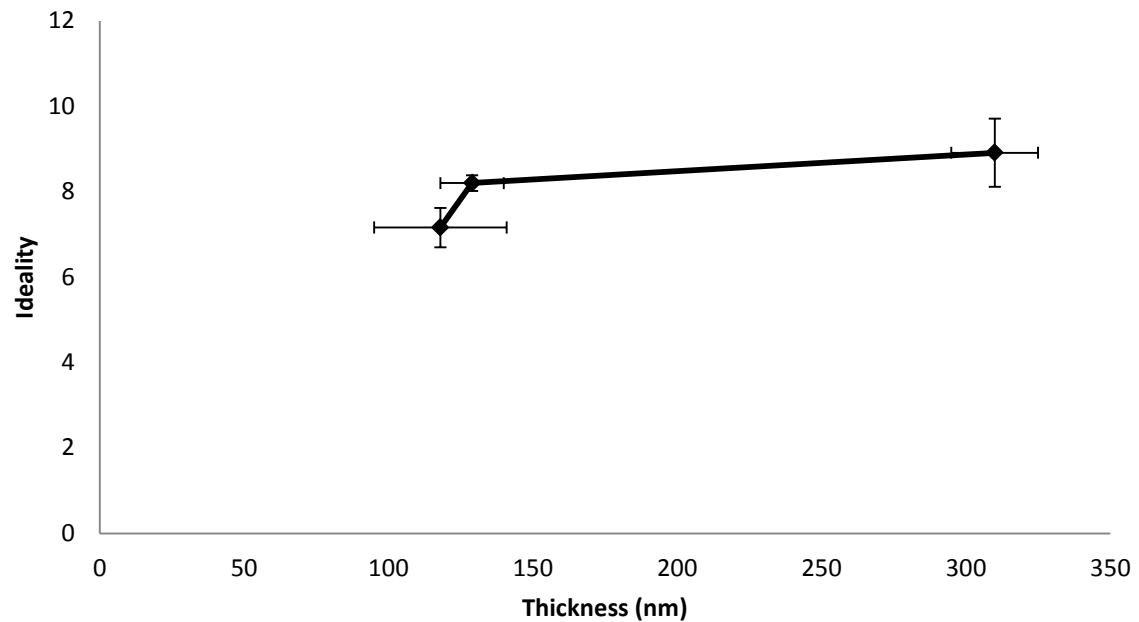


Figure 52. Ideality vs. P3HT Thickness.

Ideality values in Figure 52 ranged from 7 to 9 as thickness of the P3HT increased. The samples were fabricated with no drying time which has shown to significantly increase performance of the diodes; the lack of drying time explains the poor ideality values, despite this ideality can be seen to decrease as thickness decreases.

## 5.4. Rectification

An aim of this project was to create a diode with a rectification for comparison with an inorganic diode. The commercial Silicon diode chosen for comparison was the 1N914 fast switching Schottky diode manufactured by Vishay. The 1N914 was chosen as a benchmark because it is commonly used in low voltage switching applications such as rectifier circuits.

The plots below (Figure 53) show the forward and reverse current-voltage curves of the 1N914 diode.

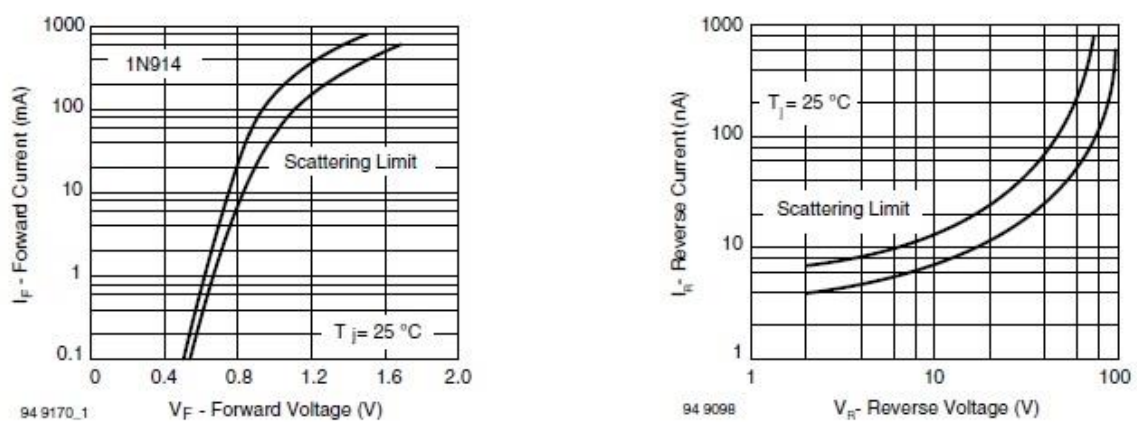


Figure 53. Current - Voltage Characteristic Curve of 1N914 silicon Schottky Diode.

The forward current at 1.2 V is 1 A and the reverse current at -1.2 V is 3 nA resulting in a rectification ratio of 300,000,000 : 1.

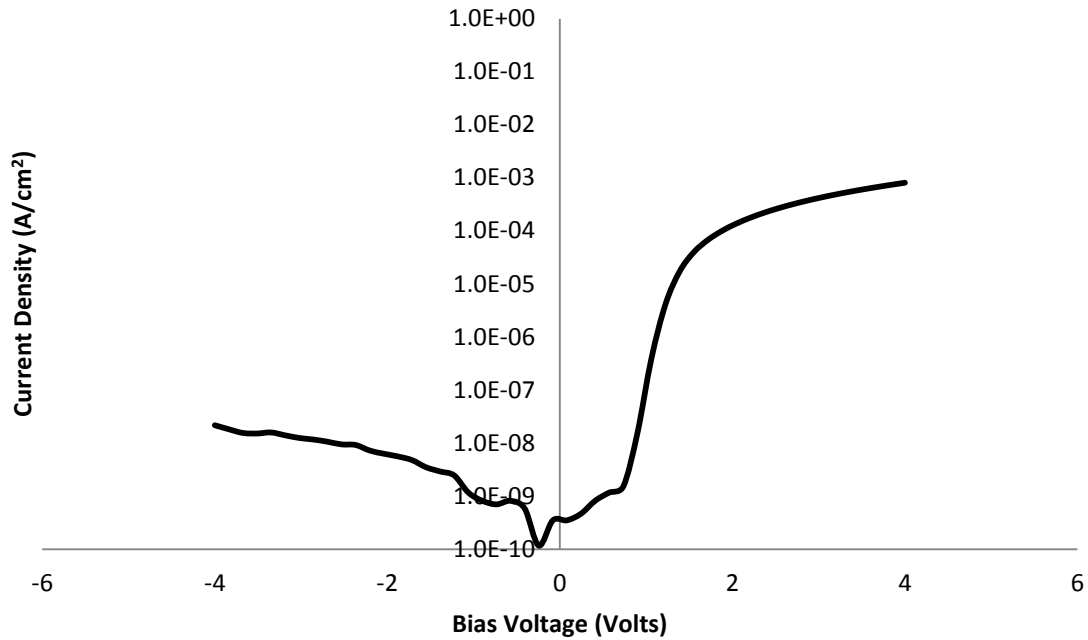


Figure 54. J-V Characteristic Curve of a diode with 5 mins drying time, annealed at 90°C for 20 mins, displaying 37,000 : 1 rectification ratio.

A current-voltage curve of a fabricated organic diode with the greatest rectification ratio at  $\pm 4$  Volts can be seen above in Figure 54. The current density at +4 volts was  $0.8 \text{ mA/cm}^2$  and at -4 volts was  $2.1 \times 10^{-5} \text{ mA/cm}^2$  resulting in a rectification ratio of 37,000 : 1.

#### 5.4.1. Half Wave Rectifier

An aim of this project was to fabricate organic diodes to rectify alternating current into direct current towards RFID applications. Two diodes with the aluminium electrode on the bottom were configured in half-wave rectifier circuits both diodes were on the same device, the only difference that diode A had a larger junction area than diode B. A circuit diagram was created in Multisim to demonstrate the testing circuit and to simulate the input and output of an idealised output for a conventional diode.

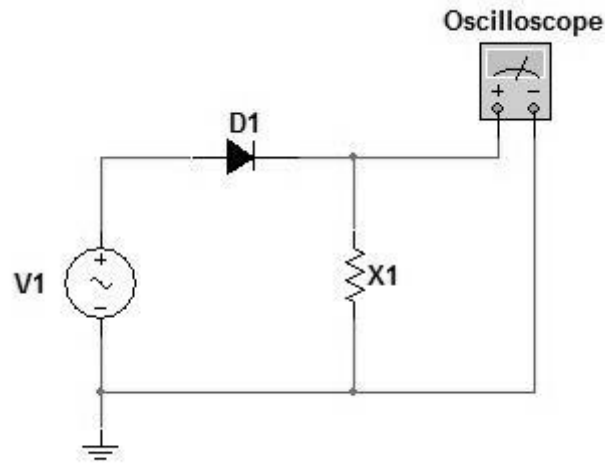


Figure 55. Diagram of half-wave rectifier circuit.

In Figure 55. The V1 is the AC voltage source, D1 is the diode under test, X1 was a resistor or capacitor, the voltage drop across X1 was measured and recorded on the oscilloscope.

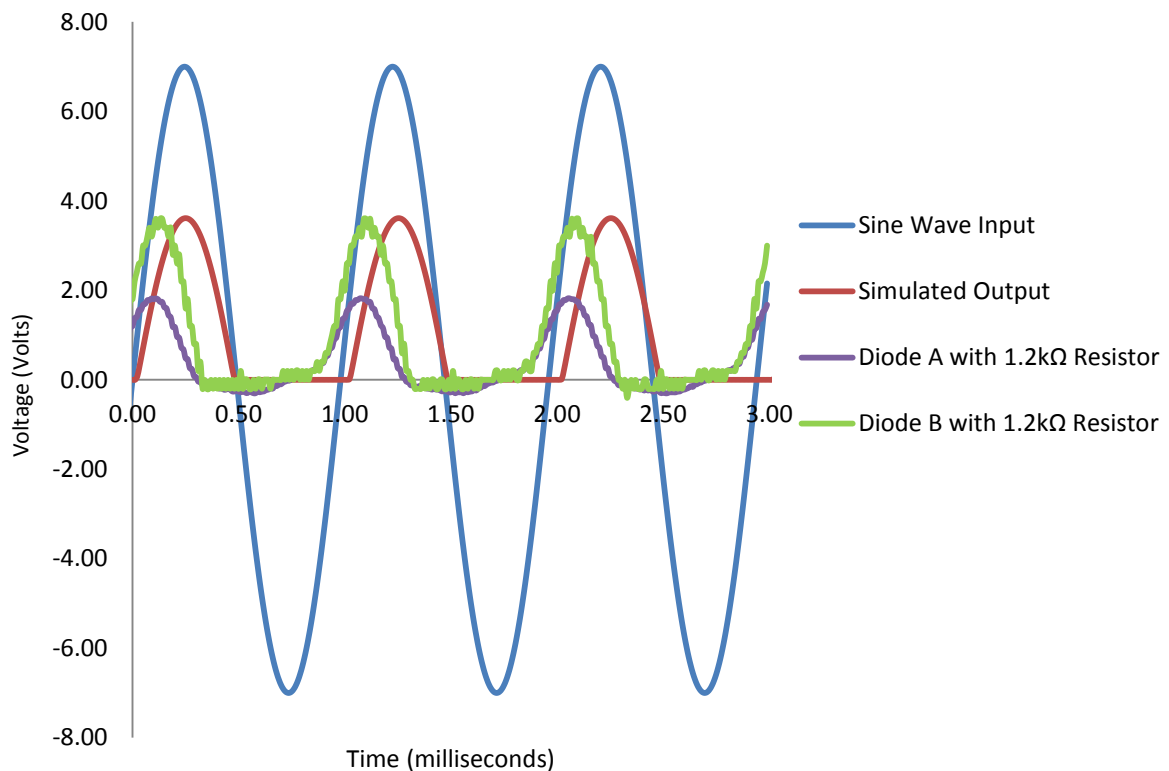


Figure 56. Half-wave Rectification of 1000Hz Sine Wave with a Resistor at position X1 in circuit and Multisim simulation of output voltage.

Figure 56 shows both the performance of both diodes A and B in negative clipper circuits. A 1.2 K $\Omega$  resistor was selected for position X1 resulting in a functioning clipper circuit, both diodes display rectification by blocking current and creating a voltage in the positive phase of the AC cycle, while allowing current to flow in the negative cycle results a small voltage.

At 1000Hz diode A and B resulted in a peak voltage of 1.7 Volts and 3.4 Volts respectively. The positive phase ( $V_{in} > 0$ ) voltage peak is greater for diode B because it has a lower reverse current, more effectively blocking the current, and causing a larger voltage difference. The negative phase ( $V_{in} < 0$ ) peak output voltage for diode A is greater than diode B due to the larger turn on voltage as a result of the smaller diode area.

The simulated output in Figure 56 demonstrates a device with no parasitic capacitance. The fabricated organic diodes have similar parasitic capacitance which causes the phase of the output voltage peaks to be shifted to the left.

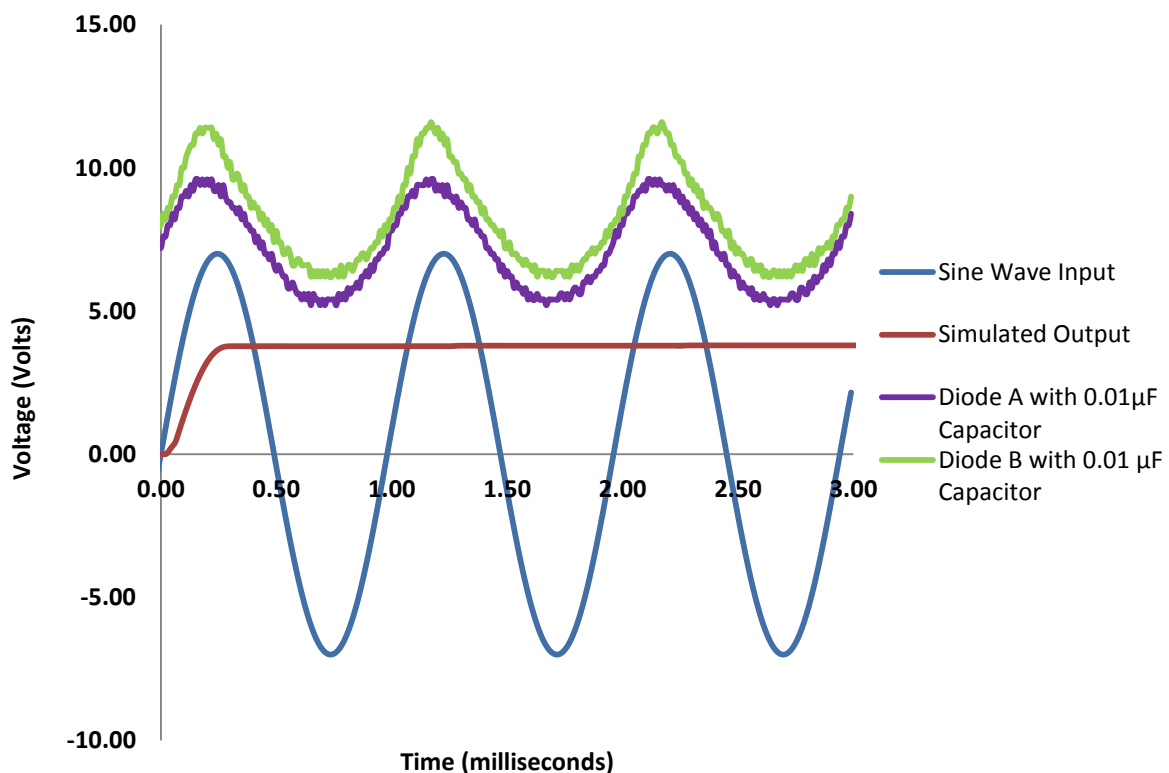


Figure 57. Half-Wave Rectification of 1000Hz Sine Wave with a Capacitor in Circuit and Multisim simulation of output voltage.

Organic diodes A and B perform rectification of 30 Volt peak to peak, 1000 Hz AC signal into DC voltage as shown in Figure 57. Diode 2 with a larger junction area resulted in a larger DC voltage of 8.4 Volts RMS, while diode 1 resulted in 7.3 Volts RMS,

Ripple of the output voltage is a product of the half wave rectification, which is due to the capacitor being discharged by the organic diode in reverse bias and charging again when the forward biased. When the input waveform falls below the DC peak voltage stored on the capacitor, the diodes bias is reversed, blocking current flow from capacitor back to the source. Thus, the capacitor retains the peak value even as the waveform drops to zero. Half-wave rectification was achieved with the organic diodes.

The diode blocks current when it is reversed biased, charging the capacitor to the waveform peak. Charging of the capacitor up from zero volts is not seen in the output voltage of diodes A and B because the oscilloscope captures the wave function once it is established, not when the circuit is first connected. The fabricated organic diodes successfully rectified 1000Hz alternating current to direct current in peak voltage and clipper circuits.

## 6. Conclusions

Diodes with a rectification value of  $7.49 \times 10^5 : 1$  were successfully fabricated for planar gold - poly(3-hexylthiophene-2,5-diyl) – aluminium diodes, with a best performing device fabricated in the inert environment of the glove-box spin coated from a 1,2 – dichlorobenzene solution with 5 mins drying time, annealed at  $90^\circ\text{C}$  for 20 mins, with an ideality factor of 2.11.

The performance of diodes in a rectification circuits is defined by their electrical properties. The impact of fabrication and testing parameters on the key electrical properties; series resistance, shunt resistance, rectification ratio and ideality was therefore investigated. Electrical properties of diodes fabricated under inert conditions were generally shown to result in superior performance over ambient fabricated diodes.

Figure 15 shows the annealing fabrications parameters; drying time, annealing temperature and annealing time. The drying time had the greatest impact on the electrical properties of the device; reducing the series resistance by three (3) orders of magnitude from  $46 \text{ K } \Omega$  (zero minutes) to  $253 \text{ } \Omega$  at 10 minutes. An improved series resistance of  $101 \text{ } \Omega$  was observed at five (5) minutes drying time. The shunt resistance increased for diodes annealed in air from  $18.6 \text{ M}\Omega$  at zero minutes to  $89.3 \text{ M}\Omega$  at 10 minutes improving the performance of the diodes; however the shunt resistance was significantly lower for devices annealed under inert conditions at only  $85 \text{ k}\Omega$ . Rectification ratio is affected by the two resistances and resulted in an increase from a barely functioning diode at  $15 : 1$  to  $1440 : 1$  for air fabricated devices, and inert devices performed better with  $629 : 1$  rectification ratio at five (5) minutes drying time. These performance improvements from increased drying time are most likely due to reorganisation of the polymer chains. Higher annealing temperatures displayed improvements in the series resistance of both air and inert fabricated devices, with air devices reducing from  $10 \text{ k}\Omega$  range at  $70^\circ\text{C}$  to below  $100 \text{ } \Omega$  above  $110^\circ\text{C}$ , additionally inert devices series resistance began at  $101 \text{ } \Omega$  at  $70^\circ\text{C}$  and reduced linearly to  $24.6 \text{ } \Omega$  at  $135^\circ\text{C}$ . However, it appears that most of the improvement in electrical properties has occurred during the drying stage of five (5) minutes and that little further improvement is observed from longer annealing times or higher annealing temperatures. Additional crystallisation may occur from higher annealing temperatures and times due to reduction of intra-chain forces but no improvement in diode performance is observed.

A test of encapsulating devices made in controlled atmosphere was carried out to investigate the effects of oxygen and water on this system. It was observed that devices required some interaction with the ambient atmosphere to be activated and display any diode-type behaviour, poly(3-hexylthiophene-2,5-diyl) is an intrinsic semiconductor but requires doping to become an extrinsic semiconductor and perform as a diode. Before activation, the current density was below  $1 \times 10^{-10} \text{ A/cm}^2$ , air was admitted into the box for 1 minute and then purged with nitrogen resulting in 0.1% oxygen per volume. The device began to perform as a diode with currents in the orders of  $1 \times 10^{-9}$  -  $1 \times 10^{-4}$  Amps with an impressive rectification ratio of  $7.49 \times 10^5 : 1$ . An aluminium electrode was exposed to air for 10 minutes as it is readily oxidised, a device was prepared and tested without breaking an inert environment, but resulted in nano-amp currents with no diode-type behaviour, and was therefore discounted as the reason for device activation.

The device parameters; electrode area and polymer layer thickness were investigated. Electrode area was found to have an inversely proportional relationship with the series and shunt resistance of the devices; while the rectification and ideality were directly related to the area. The greatest performing diodes were the smallest with an area of  $(0.01 \text{ cm}^2)$  and a rectification ratio of  $1,047 : 1$ . The linear trend of the ideality with area suggested that a diode with an area of  $0.0020 \text{ cm}^2$  would have an ideality of 1, and therefore fit the Schottky diode model perfectly. The thickness of the polymer layer is critical to the electrical properties of organic diodes was thus investigated, displaying an increase in performance of thinner polymer layer diodes. The improvement is primarily due to an increase in series resistance from  $1,100 \Omega$  at  $119 \text{ nm}$  to  $12,300 \Omega$  at  $310 \text{ nm}$ , which is caused by a shorter distance travelled by the charge carriers between electrodes.

The primary aim of this project was to observe if the diodes could be used to rectify alternating current into direct current; towards the application of inexpensive RFID components. Diodes were assembled with commercial electrical components into functioning half-wave rectifiers. A DC current of  $8.4 \text{ Volts RMS}$  was achieved from a  $30 \text{ Volt peak}$  to peak AC source at  $1000 \text{ Hz}$ . Although RFID carrier frequencies range from  $135 \text{ kHz}$  to  $13.56 \text{ MHz}$ , this result shows organic diodes have promise as rectifiers for RFID.

Current RFID components are made from inorganic semiconductors which have the advantage of being a mature technology. Solution processed organic diodes may never achieve the same electrical performance as crystalline silicon; however, with the right

fabrication parameters and very controlled doping it appears quite possible to produce diodes for radio frequency identification tags.

## 7. References

1. "Gillette to Buy 500 Million EPC Tags". RFID Journal, Nov. 2002  
<[www.rfidjournal.com/articles/view?115](http://www.rfidjournal.com/articles/view?115)>.
2. Shockley, W., *The Theory of p-n Junctions in Semiconductors and p-n Junction Transistors*. Bell System Technical Journal, 1949. **28**(3): p. 435-489.
3. Sze, S.M., *Physics of Semiconductor Devices*. 1981, New York: Wiley.
4. Rhoderick, E.H., *Metal-semiconductor contacts*. Solid-State and Electron Devices, IEE Proceedings I, 1982. **129**(1): p. 1.
5. Naarmann, H., *Polymers, Electrically Conducting*. 2000: Ullmann's Encyclopedia of Industrial Chemistry.
6. Skotheim, T., *Handbook of Conducting Polymers*. 1986: Marcel Dekker, Inc.
7. *Nobel Prize in Chemistry 2000*. 2010 [cited 2010 26-10]; Available from:  
[http://nobelprize.org/nobel\\_prizes/chemistry/laureates/2000/](http://nobelprize.org/nobel_prizes/chemistry/laureates/2000/).
8. Brütting, W., *Introduction to the Physics of Organic Semiconductors*, in *Physics of Organic Semiconductors*. 2006, Wiley-VCH Verlag GmbH & Co. KGaA. p. 1-14.
9. Katz, H. and J. Huang, *Thin-Film Organic Electronic Devices*. Annual Review of Materials Research, 2009. **39**: p. 71.
10. Moge, M., et al., *Fabrication and characterization of Schottky barrier diodes with tetracyanoquinodimethane doped with bis ( P-naphthyl ) -tetrathiafulvalene*. Synthetic Metals, 1996. **82**: p. 97.
11. Abdou, M.S.A., et al., *Interaction of Oxygen with Conjugated Polymers: Charge Transfer Complex Formation with Poly(3-alkylthiophenes)*. Journal of the American Chemical Society, 1997. **119**(19): p. 4518-4524.
12. Kozlov, O.V. and S.A. Zapunidi, *Reversible oxygen doping of conjugated polymer and its dedoping studied by Mott-Schottky analysis*. Synthetic Metals, 2013. **169**(1): p. 48-54.
13. Kline, R.J., et al., *Controlling the Field-Effect Mobility of Regioregular Polythiophene by Changing the Molecular Weight*. Advanced Materials, 2003. **15**(18): p. 1519-1522.
14. Yang, H., et al., *Out-of-plane carrier transport in conjugated polymer thin films: Role of morphology*. Journal of Physical Chemistry C, 2013. **117**(19): p. 9590-9597.
15. Duong, D.T., M.F. Toney, and A. Salleo, *Role of confinement and aggregation in charge transport in semicrystalline polythiophene thin films*. Physical Review B, 2012. **86**(20): p. 205205.
16. Huang, B., et al., *Effect of Thickness-Dependent Microstructure on the Out-of-Plane Hole Mobility in Poly(3-Hexylthiophene) Films*. ACS Applied Materials & Interfaces, 2012. **4**(10): p. 5204-5210.
17. Narula, A. and R. Singh, *Junciton Properties of Aluminium / Polypyrrole (Polypyrrole Derivatives) Schottky Diodes*. Applied Physics Letters, 1997. **71**(19): p. 2845.
18. Friend, R.H., C.A. Jones, and J.H. Burroughes, *New semiconductor device physics in polymer diodes and transistors*. Nature, 1988. **335**: p. 137.
19. Cui, T., G. Liang, and K. Varahramyan, *Fabrication and electrical characteristics of polymer-based Schottky diode*. Solid-State Electronics, 2003(47): p. 691.
20. Kang, C.-m., et al., *Frequency analysis on poly(3-hexylthiophene) rectifier using impedance spectroscopy*. Thin Solid Films, 2009. **518**(2): p. 889-892.
21. Kang, K., et al., *Performance enhancement of polymer Schottky diode by pentacene*. Thin Solid Films, 2009. **517**: p. 6096.
22. Gupta, R.K. and R.A. Singh, *Junction Properties of Schottky diode based on composite organic semiconductors*. Journal of Materials Science: Materials in Electronics, 2005. **16**: p. 253.

23. Cheung, S.K. and N.W. Cheung, *Extraction of Schottky diode parameters from forward current-voltage characteristics*. Applied Physics Letters, 1986. **49**(2): p. 85-87.
24. Norde, H., *A modified forward I-V plot for Schottky diodes with high series resistance*. Journal of Applied Physics, 1979. **50**(7): p. 5052-5053.
25. Sato, K. and Y. Yasumura, *Study of forward I-V plot for Schottky diodes with high series resistance*. Journal of Applied Physics, 1985. **58**(9): p. 3655-3657.
26. Ho, X., et al., *Theoretical and experimental studies of Schottky diodes that use aligned arrays of single-walled carbon nanotubes*. Nano Research, 2010. **3**(6): p. 444-451.
27. Chiang, K.Y., et al. *Modeling the capacitance-voltage characteristics of organic Schottky diode in the forward bias*. 2006. Boston, MA.
28. Hyun Kim, C., et al., *Modeling the low-voltage regime of organic diodes: Origin of the ideality factor*. Journal of Applied Physics, 2011. **110**(9): p. 093722.
29. Roman, L., M. Berggren, and O. Inganäs, *Polymer diodes with high rectification*. Applied Physics Letters, 1999. **75**(22): p. 3557.
30. Zehe, A., et al., *Electrical Conductivity of Tetrathiafulvalene-9-Dicyano-methylene-2,4,5,7-tetrafluorene(TTF-DT4NF)*. Crystal Research Technology, 1993. **28**(6): p. 881.
31. Adachi, C., et al., *Extremely-high-density carrier injection and transport over 1000 A/cm<sup>2</sup> into organic thin films*. Applied Physics Letters, 2005. **86**: p. 083502.
32. Steudel, S., et al., *Comparison of organic diode structures regarding high-frequency rectification behavior in radio-frequency identification tags*. Journal of Applied Physics, 2006. **99**: p. 114519.
33. Baude, P.F., et al., *Pentacene-based radio-frequency identification circuitry*. Applied Physics Letters, 2003. **82**(22): p. 3964.
34. Ma, L., J. Ouyang, and Y. Yang, *High-speed and high-current density C60 diodes*. Applied Physics Letters, 2004. **84**(23): p. 4786-4788.
35. Gupta, R.K. and R.A. Singh, *Junction Properties of Schottky Diode Based on Composite Organic Semiconductors: Polyaniline-Polystyrene System*. Journal of Polymer Research, 2004. **11**: p. 269.
36. Miyaucki, S., et al., *Schottky Barrier formation between polypyrrole and Indium*. Synthetic Metals, 1987. **18**: p. 689.
37. Miyaucki, S., et al., *Junction Properties between Indium and Doped Polypyrrole*. Synthetic Metals, 1989. **28**: p. C691.
38. Ahmad, Z. and M. Sayyad, *Extraction of electronic parameters of Schottky diode based on an organic semiconductor methyl-red*. Physica E, 2009. **41**: p. 641.
39. Speakman, S.P., et al., *High performance organic semiconducting thin films: Ink jet polythiophene [rr-P3HT]*. Organic Electronics, 2001. **65**: p. 73.
40. Nolasco, J.C., et al., *Extraction of poly (3-hexylthiophene) (P3HT) properties from dark current voltage characteristics in a P3HT/n-crystalline-silicon solar cell*. Journal of Applied Physics, 2010. **107**(4): p. 044505.
41. Myny, K., et al., *An integrated double half-wave organic Schottky diode rectifier on foil operating at 13.56 MHz*. Applied Physics Letters, 2008. **93**: p. 093305.
42. Clarke, T.C., et al., *Properties of metal/polyacetylene Schottky barriers*. Journal of Applied Physics, 1980. **52**(2): p. 869.
43. Etoh, S. and H. Koezuka, *Schottky barrier type diode with an electrochemically prepared copolymer having pyrrole and N-methylpyrrole units*. Journal of Applied Physics, 1983. **54**(5): p. 2511.
44. Gupta, R., et al., *Metal Semiconductive Polymer Schottky Device*. Applied Physics Letters, 1990. **58**(1): p. 51-52.
45. Steudel, S., et al., *50 MHz rectifier based on an organic diode*. Nature Materials, 2006. **4**: p. 598.
46. Voss, D., *Cheap and cheerful circuits*. Nature, 2000. **407**: p. 442.

47. Schmid, G., et al., *Pentacene organic transistors and ring oscillators on glass and on flexible polymeric substrates*. Applied Physics Letters, 2003. **82**(23): p. 4175.
48. Lilja, K., et al., *Gravure printed organic rectifying diodes operating at high frequencies*. Organic Electronics, 2009. **10**: p. 1011.
49. Chang, J.-F., et al., *Enhanced Mobility of Poly(3-hexylthiophene) Transistors by Spin-Coating from High-Boiling-Point Solvents*. Chemistry of Materials, 2004. **16**(23): p. 4772-4776.
50. Keithley *Keithley 2400 Series SourceMeter® SMU Instruments*.
51. Kang, C.M., Y. Hong, and C. Lee, *Frequency performance optimization of flexible pentacene rectifier by varying the thickness of active layer*. Japanese Journal of Applied Physics, 2010. **49**(5 PART 2): p. 05EB071-05EB074.
52. Weast, R.C., *CRC Handbook of Chemistry and Physics*. 56 ed. 1975: CRC Press.
53. Keithley *Making Precision Low Current and High Resistance Measurements*. 2014.
54. Kaneto, K., M. Ujimoto, and W. Takashima. *Photoinduced memory effects based on poly(3-hexylthiophene) and Al interface*. 2005. Boston, MA.
55. Dwivedi, A.D.D., et al., *A proposed organic Schottky barrier photodetector for application in the visible region*. Current Applied Physics, 2010. **10**(3): p. 900-903.
56. Sahingoz, R., et al., *The determination of the conduction mechanism and extraction of diode parameters of ITO/PEDOT-PSS/POLYMER/Al heterojunction diode*. Optical Materials, 2006. **28**(8-9): p. 962-965.
57. Müller, C., *On the Glass Transition of Polymer Semiconductors and Its Impact on Polymer Solar Cell Stability*. Chemistry of Materials, 2015. **27**(8): p. 2740-2754.
58. Agarwala, V.K. and T. Fort Jr, *Nature of the stable oxide layer formed on an aluminum surface by work function measurements*. Surface Science, 1976. **54**(1): p. 60-70.
59. Assadi, A., et al., *Field-effect mobility of poly(3-hexylthiophene)*. Applied Physics Letters, 1988. **53**(3): p. 195-197.
60. Bao, Z., A. Dodabalapur, and A. Lovinger, J, *Soluble and processable regioregular poly(3-hexylthiophene) for thin film field-effect transistor applications with high mobility*. Applied Physics Letters, 1996. **89**(4108).
61. Singh, T.B. and N.S. Sariciftci, *PROGRESS IN PLASTIC ELECTRONICS DEVICES*. Annual Review of Materials Research, 2006. **36**(1): p. 199-230.